COMILLAS
UNIVERSIDAD PONTIFICIA
ICAI

GRADO EN INGENIERÍA EN TECNOLOGÍAS DE TELECOMUNICACIÓN

TRABAJO FIN DE GRADO

The combustion process in a scramjet. Experimental study of the effectiveness of supersonic waves in the combustion of a scramjet conducted in a mini wind tunnel at the University of Minnesota.

Autor: Santiago José Bercedo Posada

Director: Sayan Biswas

Madrid

Declaro, bajo mi responsabilidad, que el Proyecto presentado con el título

The combustion process in a scramjet. Experimental study of the effectiveness of supersonic waves in the combustion of a scramjet conducted in a mini wind tunnel at the University of Minnesota.

en la ETS de Ingeniería - ICAI de la Universidad Pontificia Comillas en el

curso académico 2022/23 es de mi autoría, original e inédito y

no ha sido presentado con anterioridad a otros efectos.

El Proyecto no es plagio de otro, ni total ni parcialmente y la información que ha sido

tomada de otros documentos está debidamente referenciada.

Fdo.: Santiago José Bercedo Posada Fecha: 02/ 07/2023

Autorizada la entrega del proyecto

EL DIRECTOR DEL PROYECTO

Fdo.: Sayan Biswas Fecha: 12/ 07/ 2023

COMILLAS
UNIVERSIDAD PONTIFICIA
ICAI

GRADO EN INGENIERÍA EN TECNOLOGÍAS DE TELECOMUNICACIÓN

TRABAJO FIN DE GRADO

The combustion process in a scramjet. Experimental study of the effectiveness of supersonic waves in the combustion of a scramjet conducted in a mini wind tunnel at the University of Minnesota.

Autor: Santiago José Bercedo Posada

Director: Sayan Biswas

Madrid

Acknowledgments

This research greatly benefited from the help of Gabe Holum, without which this work would not have been possible. His contributions in helping to run the experiments and analyzing the data were essential.
I would also like to express my gratitude to Professor Biswas for the trust he has placed in me to use the facilities of the Thomas E. Murphy Engine Research Lab.
I would like to thank my family, especially my parents, and all my friends for all the support they have given me all these years.

EL PROCESO DE COMBUSTIÓN EN UN SCRAMJET. ESTUDIO EXPERIMENTAL DE LA EFICACIA DE LAS ONDAS SUPERSÓNICAS EN LA COMBUSTIÓN DE UN SCRAMJET REALIZADO EN UN MINI TÚNEL DE VIENTO DE LA UNIVERSIDAD DE MINNESOTA.

Autor: Bercedo Posada, Santiago José.
Director: Biswas, Sayan.
Entidad Colaboradora: University of Minnesota

RESUMEN DEL PROYECTO

En el laboratorio de la Universidad de Minnesota se ha llevado a cabo un estudio experimental para analizar el comportamiento de un chorro líquido inyectado en un flujo supersónico con el objetivo de investigar nuevos métodos que fomenten a la atomización y mezcla de dicho chorro con el aire.

Palabras clave: ondas supersónicas, altura de penetración, chorro, cuña, túnel de viento.

1. Introducción.

Los *scramjets* son motores diseñados para operar a velocidades supersónicas desde Mach 5 hasta Mach 15, que aprovechan la velocidad del vehículo para comprimir el aire antes de su entrada en la cámara de combustión. Estos motores pueden estar alimentados por diferentes tipos de combustible, como hidrógeno gaseoso o hidrocarburos líquidos. Los *scramjets* alimentados por combustibles líquidos se enfrentan al problema de lograr una disgregación y mezcla adecuadas del combustible con el aire en el corto tiempo de permanencia dentro de la cámara de combustión [1]. Sin ello, la combustión no es tan eficiente como podría llegar a ser [2]. Uno de los mecanismos más prometedores para logar una buena mezcla es la inyección de un chorro de combustible líquido en el flujo cruzado supersónico. Esto es lo que se conoce como LJISC (*liquid jet in supersonic crossflow*).

2. Problema.

La problemática del LJISC se muestra en la siguiente imagen recuperada de [3].

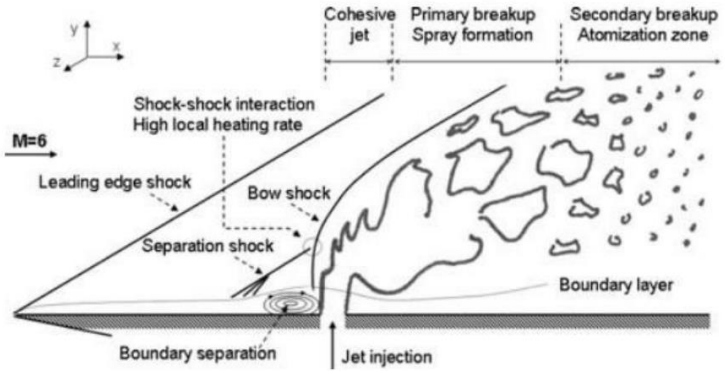

LJISC [3].

El combustible es inyectado y golpeado por el aire que viaja a altísimas velocidades. Uno de los parámetros más estudiados para conseguir una buena mezcla es la altura de penetración del chorro de combustible líquido. Cuanto mayor sea la altura de penetración, mejor será la combustión [4].

A lo largo de los años se han realizado numerosos estudios experimentales acerca del tema; sin embargo, los resultados son todavía muy inconclusos y se necesita más investigación.

Este estudio sigue como ejemplo el experimento realizado por Sebastian *et al*. [5] en el año 2022. En él, se añade una cuña que funciona como generador de ondas (*shock generator*) en la parte superior del túnel de viento. El objetivo es crear una nueva onda oblicua que incida en la parte fuerte de la *bow shock*, y así conseguir aumentar su altura de penetración.

Sin embargo, este trabajo se realiza con un diseño de cuña diferente. El esquema se muestra en la siguiente imagen, donde OS hace referencia a la *Oblique Shock* creada por el *shock generator* y BS hace referencia a la *Bow Shock*.

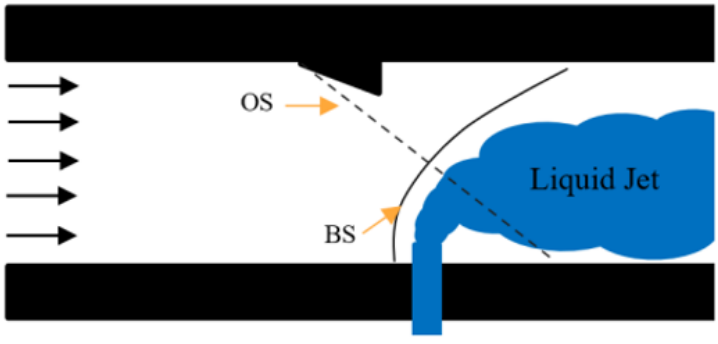

Esquema de la sección de prueba.

3. Descripción de las herramientas utilizadas.

El objetivo es estudiar el efecto que tiene el *shock generator* sobre la altura de penetración del líquido. Para ello se ha hecho uso de las instalaciones del Thomas E. Murphy Engine Research Laboratory en la Universidad de Minnesota. Los experimentos se han realizado en un túnel de viento que se puede dividir en dos partes. Por un lado, el sistema de aire, a través del cual se alcanza un Mach próximo a 2; por otro lado, el sistema de agua encargado de administrar el líquido presurizado. En este experimento se ha trabajo solo con agua como líquido de prueba por cuestiones ambientales.

Se han llevado a cabo dos experimentos en los que para la toma de imágenes se ha hecho uso de las técnicas de fotografía Schlieren y de imagen directa. En el primero de ellos se comprobó el comportamiento de las ondas supersónicas a través de la fotografía Schlieren visualizando las variaciones en la densidad del fluido. En el segundo experimento se estudió el comportamiento del líquido a través de la imagen directa.

En un primer momento, ambos experimentos iban a ser estudiados a través del efecto Schlieren. Sin embargo, debido a la rápida separación de la capa límite causada por el gradiente de presión adverso, se creó una zona de recirculación que provocó que el agua del chorro se moviese aguas arriba. Como consecuencia, las gotas de agua se quedaron pegadas a las ventanas del túnel, provocando el oscurecimiento de la imagen. Por ello, el segundo experimento se estudió a través de la imagen directa.

4. Resultados.

Para conocer el ángulo óptimo de la cuña y provocar que la onda oblicua creada por ella impactase en el lugar deseado, se utilizó la fórmula en la que se relaciona el número de Mach (M) con el ángulo de la cuña (θ) y el ángulo de la onda (β) [6].

$$\tan\theta = 2\cot\beta\,\frac{M_1^2 sin^2\beta - 1}{M_1^2(\gamma + \cos 2\beta) + 2}$$

Según los resultados teóricos la situación óptima se produciría con una cuña de 19º. Sin embargo, también se diseñaron otras dos cuñas de 12º y 15º para ver las diferencias que producirían en el proceso de atomización.

En las siguientes imágenes se compara el caso base (sin la presencia de la cuña) con los otros tres.

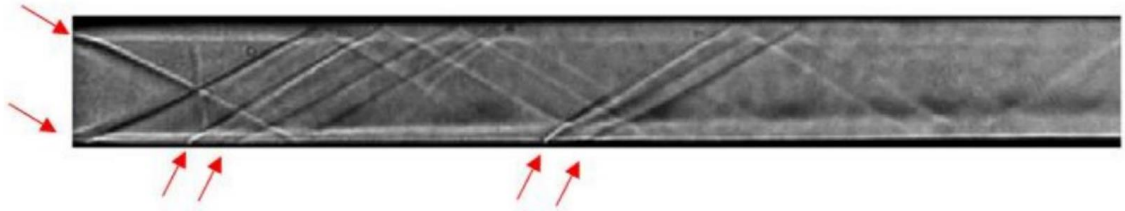

Caso base.

Las flechas rojas muestran las ondas supersónicas que se crean en la sección de prueba del túnel de viento debido a las pequeñas perturbaciones existentes en él. Las dos primeras de la izquierda son generadas por un pequeño borde que une la sección de prueba con el resto de la estructura del túnel. Las dos siguientes, en la base, son creadas por un pequeño agujero donde se encuentra ubicado un transductor de presión encargado de recoger información. Las dos últimas, más adelante, son las creadas por el agujero a través del cual el líquido es inyectado. En la imagen también se observa cómo las ondas de choque oblicuas que impactan sobre las paredes del túnel rebotan siguiendo el mismo ángulo que la onda inicial. Estas son las denominadas ondas de choque reflejadas y tienen menor intensidad que las iniciales.

Las siguientes tres imágenes muestran las ondas de choque una vez se han añadido los diferentes tipos de *shock generators.*

Cuña de 12°

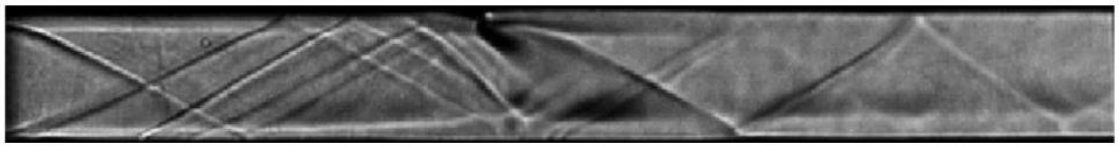

Cuña de 15°

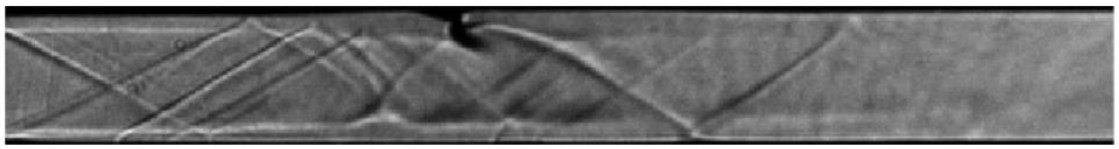

Cuña de 19°

Las imágenes muestran que cuando se añade cualquier tipo de cuña aparece una fuerte onda de choque cuyo origen se encuentra en el final de la misma. Esto puede ser fruto de la ruptura de la capa límite y las fuertes turbulencias creadas en la zona por el proceso de compresión y expansión del aire. Sin embargo, la onda de choque de interés es la formada en la parte delantera de la cuña. En el caso de la cuña de 19º, dicha onda es prácticamente inexistente. Para el caso de la cuña de 15º, parece formarse una onda de choque desprendida. Por ello, para realizar el segundo experimento se decidió utilizar simplemente la cuña de 12º, puesto que mostraba los resultados más coherentes.

Gracias al uso de ImageJ se pudieron medir los ángulos creados por las ondas y compararlos con los resultados teóricos.

	Ángulo de la onda	
Ángulo de la cuña	**Resultados teóricos**	**ImageJ**
12º	41,576º	38º
15º	45,345º	32º
19º	51,503º	36º

Tabla de resultados.

Los resultados pueden parecer muy desviados, aunque cabe destacar que pequeñas variaciones en el número de Mach implican grandes cambios en el ángulo de la onda de choque creado. Los cálculos teóricos se realizaron con un Mach 2 y en el laboratorio no siempre se llegaba a él por diferentes motivos como el progresivo consumo de los tanques de aire comprimido.

En el segundo experimento se estudió la altura de penetración del líquido. Para definir los límites del chorro se binarizó la imagen seleccionando un valor de intensidad de umbral del 18,5%. En este experimento, debido a que los vídeos fueron realizados con imagen directa y no mediante la técnica Schlieren, se desconocía el trayecto real de las ondas de choque generadas por la cuña, al igual que tampoco se pudo saber si nuevas ondas de choque habían sido generadas.

La siguiente imagen muestra, con dos líneas en rojo, una estimación del trayecto de las ondas de choque.

Estimación del trayecto de las ondas de choque.

Los resultados obtenidos en el cálculo de la altura de penetración se muestran en la siguiente gráfica.

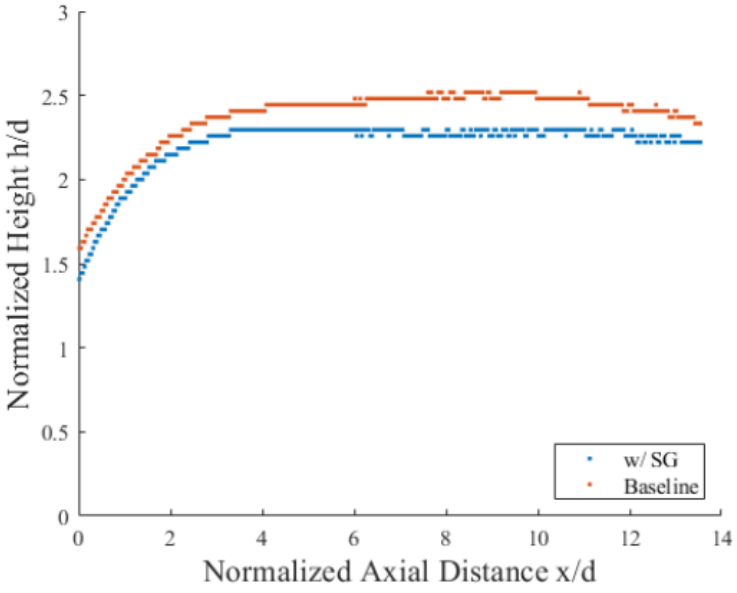

Gráfico de las alturas de penetración. (SG=Shock Generator)

Se observa como para el caso base, la altura de penetración es superior. Esto contradice los resultados obtenidos por Sebastian *et al.* [5], pero diferentes factores han de tenerse en cuenta.

En primer lugar, la onda de choque incidente no llegó a impactar en el punto más fuerte de la *bow shock*. Por el contrario, golpeó más atrás y provocó una onda de choque trasmitida y trajo como resultado una altura de penetración menor.

Al mismo tiempo, la formación de una onda de choque desde la parte trasera de la cuña pudo provocar que la altura de penetración en la parte trasera de la pluma de *spray* fuese menor. En la gráfica se muestra como a partir de x/d=4 los valores se estabilizan. Esto pudo ser una consecuencia de las pequeñas dimensiones del túnel de viento que provocaron el continuo rebote de las odas de choque trasmitidas.

5. Conclusiones.

Pese a haber obtenido resultados muy interesantes, no se pueden sacar conclusiones definitivas. Se necesita más experimentación para poder conocer el efecto real de las ondas supersónicas producidas por una cuña en el proceso de atomización de un líquido en un flujo supersónico.

Es cierto que los resultados son diferentes a los esperados, pero hay que tener en cuenta que la geometría y forma de la cuña también lo eran. Al mismo tiempo, las diferentes técnicas de visualización (en este caso, Schlieren o imagen directa) y el parámetro con el que se establecieron los límites en el chorro pueden tener importantes efectos en la altura de penetración.

De cara a futuro, resultaría interesante poder realizar el segundo experimento a través de fotografía Schlieren para ver las ondas de choque que realmente se crean. La Universidad de Minnesota se encuentra actualmente trabajando en un túnel de viento mucho más preciso y con una mayor sección de prueba para obtener mejores resultados.

La adición de un *shock generator* puede traer significativos beneficios en el proceso de combustión, pero mucha más experimentación es necesaria.

Referencias.

[1] Z. Ren, B. Wang, G. Xiang, D. Zhao y L. Zheng, «Supersonic spray combustion subject to scramjets: Progress and challenges.,» *Progress in Aerospace Sciences.*, vol. 105, pp. 40-59, 2019.

[2] C. Ghenai, H. Sapmaz y C. X. Lin, « Characterization of Aerated Liquid Jet in Subsonic and Supersonic Cross Flow.,» *AIAA journal*, 2005.

[3] J. B. Perurena, C. O. Asma, R. Theunissen y O. Chazot, «Experimental investigation of liquid jet injection into Mach 6 hypersonic crossflow.,» *Experiments in Fluids*, vol. 46, nº 3, pp. 403-417, 2009.

[4] C. Segal, Supersonic Combustion Processes, 2009.

[5] D. S. Sebastian, . S. K. Thomas y . T. Muruganandam, «Gas dynamic effects of shock interaction with the liquid jet in supersonic crossflow.,» *AIAA*, 2022.

[6] J. D. Anderson, Fundamentals of Aerodynamics, 2 ed., McGraw-Hill, Inc, 1991.

THE COMBUSTION PROCESS IN A SCRAMJET. EXPERIMENTAL STUDY OF THE EFFECTIVENESS OF SUPERSONIC WAVES IN THE COMBUSTION OF A SCRAMJET CONDUCTED IN A MINI WIND TUNNEL AT THE UNIVERSITY OF MINNESOTA.

Author: Bercedo Posada, Santiago José.
Supervisor: Biswas, Sayan.
Collaborating Entity: University of Minnesota.

ABSTRACT

An experimental study has been carried out at the laboratory of the University of Minnesota to analyze the behavior of a liquid jet injected into a supersonic crossflow with the objective of investigating new methods to promote atomization and mixing of the jet with the air.

Keywords: supersonic waves, penetration height, jet, wedge, wind tunnel.

1. Introduction.

Scramjets are engines designed to operate at supersonic speeds over a range of Mach number values between 5 and 15. These engines take advantage of the vehicle's speed to compress the air before it reaches the combustion chamber. These engines can be powered by different types of fuel such as gaseous hydrogen or liquid hydrocarbons. Liquid-fuel scramjets face the problem of achieving a proper fuel disaggregation and mixing with the air in the short residence time inside the combustion chamber [1]. Without it, combustion is not as efficient as it could be [2]. One of the most promising mechanisms to achieve a good mixing is the injection of the liquid jet of fuel into the supersonic crossflow. This is known as LJISC (liquid jet in supersonic crossflow).

2. Problem.

LJISC problem is shown in the following image retrieved from [3].

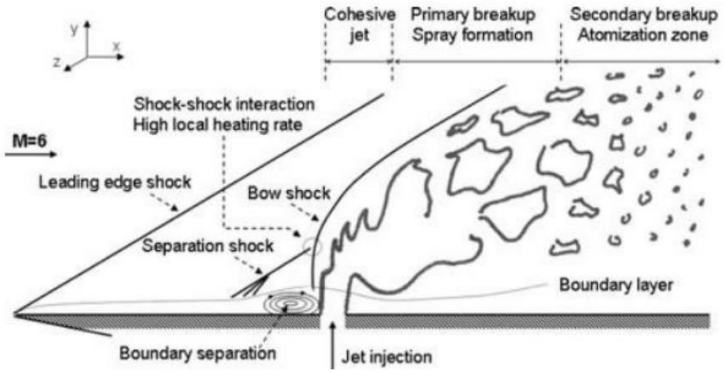

LJISC [3].

The fuel is injected and hit by the air traveling at ultra-high speeds. One of the most studied parameters to achieve a good mixing is the penetration height of the liquid jet. The higher the penetration height, the better the combustion [4].

Numerous experimental studies have been conducted on the subject over the years, however, the results are still very inconclusive, and more research is needed.

This study uses as a model experiment, the experiment performed by Sebastian *et al*. [5] in 2022. In it, a wedge that worked as a shock generator was added at the top of the wind tunnel. The objective was to create a new oblique wave that impacted on the strong part of the bow shock, thus increased its penetration height.

However, this study was performed with a different wedge design. The scheme is shown in the following image where OS refers to the Oblique Shock created by the shock generator and BS refers to the Bow Shock.

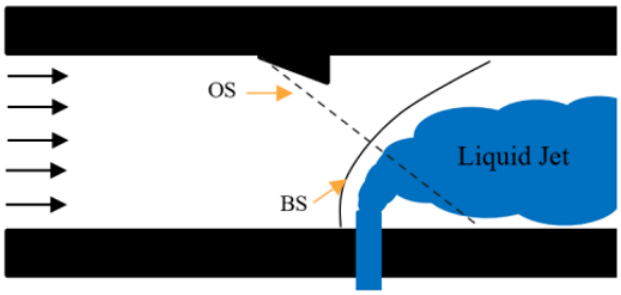

Schematic diagram of the test section.

3. Description of the tools used.

The objective of the project is to study the penetration height of a liquid jet when adding a shock generator. For this purpose, the facilities of the Thomas E. Murphy Engine Research Laboratory at the University of Minnesota were used extensively. The experiments were

carried out in a wind tunnel that can be divided into two parts for its better understanding. The air system, through which a Mach close to 2 was reached. And the water system, in charge of administering the pressurized liquid. In this experiment, only water was used as the test liquid due to environmental reasons.

Two experiments were carried out. For the capture of images, Schlieren imaging and direct imaging were used. In the first one, the behavior of supersonic waves was analyzed by means of Schlieren photography, visualizing the variations in fluid density. In the second experiment, the behavior of the fluid was studied through direct imaging.

Initially, both experiments were to be studied through the Schlieren effect. However, due to the rapid separation of the boundary layer caused by the adverse pressure gradient, a recirculation zone was created which caused the jet water to move upstream causing the water droplets to stick to the wind tunnel windows causing the image to darken. To prevent this, in the second experiment direct imaging was used.

4. Results.

To determine the optimum angle of the wedge so that the oblique wave created by it impacted at the desired location, the formula relating the Mach number (M), the wedge angle (θ) and the angle of the wave (β) was used [6].

$$\tan\theta = 2\cot\beta\,\frac{M_1^2 sin^2\beta - 1}{M_1^2(\gamma + \cos 2\beta) + 2}$$

According to the theoretical results, the optimum situation would occur with the 19º wedge. However, two other wedges of 12º and 15º were also designed to see the differences they would produce in the atomization process.

The following images compare the baseline case (without the presence of the shock generator) with the other three cases.

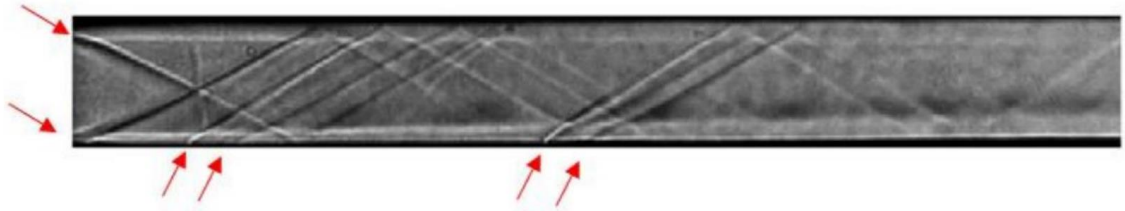

Baseline.

The red arrows show the supersonic waves that were created in the test section of the wind tunnel due to small disturbances in it. The first two, on the left, were generated by a small edge that joined the test section with the rest of the tunnel structure. The next two, at the base, were created by a small hole where a pressure transducer was located to collect information. The last two, further along the base, were created by the hole through which the liquid was injected. The image also shows how the oblique shock waves that impacted on the wind tunnel walls rebounded following the same angle as the initial wave. These are the so-called reflected shock waves and have lower intensity than the initial ones.

The following three images show the shock waves of the test section once the different shock generators were added.

Wedge of 12°

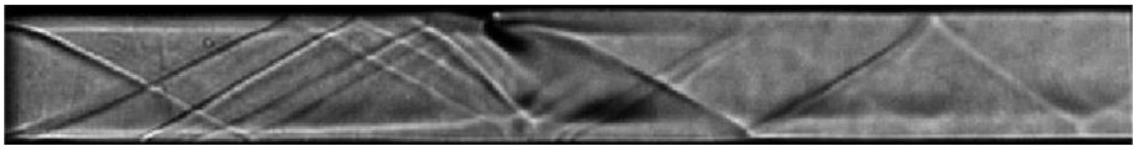

Wedge of 15°

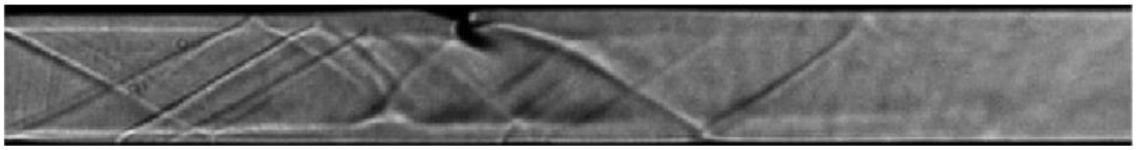

Wedge of 19°

The images show that when any type of wedge was added, a strong wave appeared whose origin was at the end of the wedge. This may have been a result of boundary layer rupture and the strong turbulence created in the area by the process of air compression and

expansion. However, the wave of interest was the one formed at the front of it. In the case of the 19º wedge, such a wave was practically non-existent. In the case of the 15º wedge, a detached shock wave seemed to be formed. Therefore, for the second experiment it was decided to simply use the 12° wedge since it showed the most consistent results.

Using ImageJ, the angles created by the waves could be measured and compared with the theoretical results.

	Wave Angle	
Wedge Angle	**Theoretical results**	**ImageJ**
12º	41.576º	38º
15º	45.345º	32º
19º	51.503º	36º

Table of results.

The theoretical results were very different from the practical ones. However, it is worth noting that small variations in the Mach number have large changes in the wave angle created. Theoretical calculations were made with a Mach 2 and in the laboratory, it was not always reached for different reasons such as the consumption of the compressed air tanks.

In the second experiment, the penetration height of the liquid was studied. To define the jet boundaries, the image was binarized by selecting a threshold intensity value of 18.5%. In this experiment, because the videos were made with direct imaging and not using the Schlieren technique, the actual path of the shock waves generated by the wedge was not known, nor was it possible to know if new shock waves had been generated.

The following image shows, with two red lines, an estimate of the shock wave path.

Estimation of the shock wave path.

The penetration height results are shown in the following graph.

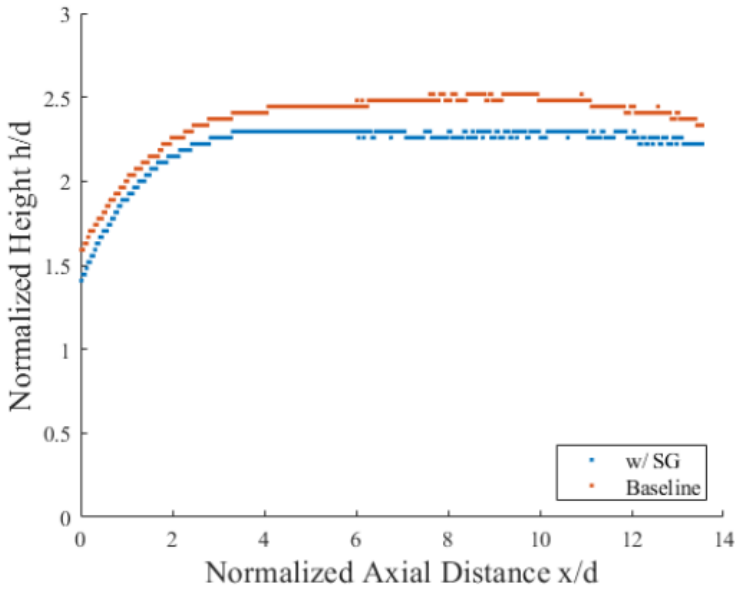

Graph of the penetration height. (SG=Shock Generator)

It is observed that for the baseline case, the penetration height is higher. This contradicts the results obtained by Sebastian *et al*. [5] but different factors must be taken into account.

First, the incident shock wave did not hit the strongest point of the bow shock wave. Instead, it hit further back and caused a transmitted shock wave, resulting in a lower penetration height.

At the same time, the formation of a shock wave from the rear of the wedge may have caused the penetration height at the downstream of the spray plume to be lower. The plot shows how from *x/d*=4 the values stabilize. This could be due to the small dimensions of the wind tunnel which caused the continuous rebound of the transmitted shock waves.

5. Conclusions

Although very interesting results have been obtained, no definitive conclusions can be drawn, and more experimentation is needed to know the real effect of supersonic waves produced by a wedge in the process of atomization of a liquid in a supersonic crossflow.

It is true that the results are different than expected but it must be taken into account that the geometry and shape of the wedge was also different. At the same time, the different visualization techniques (in this case, Schlieren and direct imaging) and the parameter with which the boundaries are set in the liquid jet can have important effects on the penetration height.

In the future, it would be interesting to be able to perform the second experiment through Schlieren photography to see the shock waves that are actually created. The University of Minnesota is currently working on a much more accurate wind tunnel with a larger test section for better results.

The addition of a shock generator can bring significant benefits in the combustion process, but much more experimentation is needed.

6. References

[1] Z. Ren, B. Wang, G. Xiang, D. Zhao y L. Zheng, «Supersonic spray combustion subject to scramjets: Progress and challenges.,» *Progress in Aerospace Sciences.*, vol. 105, pp. 40-59, 2019.

[2] C. Ghenai, H. Sapmaz y C. X. Lin, « Characterization of Aerated Liquid Jet in Subsonic and Supersonic Cross Flow.,» *AIAA journal,* 2005.

[3] J. B. Perurena, C. O. Asma, R. Theunissen y O. Chazot, «Experimental investigation of liquid jet injection into Mach 6 hypersonic crossflow.,» *Experiments in Fluids*, vol. 46, nº 3, pp. 403-417, 2009.

[4] C. Segal, Supersonic Combustion Processes, 2009.

[5] D. S. Sebastian, . S. K. Thomas y . T. Muruganandam, «Gas dynamic effects of shock interaction with the liquid jet in supersonic crossflow.,» *AIAA*, 2022.

[6] J. D. Anderson, Fundamentals of Aerodynamics, 2 ed., McGraw-Hill, Inc, 1991.

Table of Contents

Index of figures

Index of images

Index of graphs

Index of tables

Chapter 1. INTRODUCTION

Before starting to develop the work in a more technical way, it is essential to put the reader in context about the technological evolution that aviation has undergone over the years in order to understand the reason for this study.

1.1 AVIATION

It was in 1903, in North Carolina, when the Wright brothers successfully achieved controlled flight in a heavier-than-air aircraft. The first aircraft in question was powered by a 4-cylinder, 16-horsepower gasoline engine [7] . From then on, the world of aviation experienced great advances largely due to technological development.

The first airplanes were made of wooden frames and cloth and were powered by very rudimentary engines. However, it was only a short time before aircraft were designed and built with metal structures that were used for armament purposes, as well as for transporting goods and people [7].

Today, aviation is a common means of transportation with highly sophisticated technologies that allow automated flights through precise navigation systems.

In 1940, research began on supersonic aircraft capable of breaking the sound barrier. Traditional engines and propellers were not able to meet the requirements, but the technological impulse of the Second World War opened the doors to jet engines and the construction of the jet. Captain Charles Yeager broke the sound barrier for the first time in 1947, leading to the use of Mach as an effective unit of measurement of speed. The Mach number is a relative measure which relates the speed of an object to the speed of sound in the medium in which the object is moving [7] .

The development of supersonic aircraft for military and commercial purposes, such as passenger transport with the Concorde, began. The ambition to achieve something better is

inherited in human beings; thus, today 's aviation focuses on faster flights with less environmental impact.

In this study, it will be analyzed how scramjet-powered vehicles work for reaching hypersonic speeds, in other words, exceeding Mach 5. But the real aim of it, is to analyze how the effectiveness of combustion in a scramjet engine can be increased.

Compared to rocket-powered vehicles, the great advantage of these vehicles is that they are similar to airplanes and aim to achieve greater affordability and safety in hypersonic transportation.

1.2 STATE OF THE ART

It is necessary to understand the meaning of scramjet thoroughly, and for this purpose, it is inevitable to define the concept of ramjet. Ramjets are engines that achieve their propulsion through the subsonic combustion of fuel in a stream of compressed air produced by the aircraft's forward speed in consideration. In contrast, in scramjets the flow is maintained supersonic throughout the engine. These engines operate over a range of Mach number values between 5 and 15 [8].

These aircraft are not made up of moving or rotating parts, so they generally need the impulse of other aircraft to reach the necessary speeds to become operational.

The technology used in supersonic combustion ramjets is very recent, it has only been studied since the 1950s, and there is still much to be known. Tests have been mainly carried out in wind tunnels or computer systems. Few real flight tests have been performed and ever fewer have been successful.

Scramjets can use different types of fuel, including gaseous hydrogen and liquid hydrocarbon fuels.

Hydrogen is the principal and most feasible fuel used in these aircrafts due to its broad flammability range, high diffusivity, and minimum ignition energy. On the other hand,

hydrocarbon fuels give rise to much more challenges when talking about combustion [9], but are beneficial because they can be stored in their liquid form without cryogenic systems.

Liquid-fueled scramjets face the problem of achieving proper fuel disaggregation at a molecular level and mixing, in the few milliseconds in which combustion takes place [4]. Without complete mixing, the process is not as efficient as it could be. Thus, the present study will focus on analyzing the problem of liquid injection in supersonic crossflow (LJISC, liquid jet in supersonic crossflow), in other words, the effects of injecting the fuel perpendicular to the supersonic stream.

Experimental work exists on the subject in question. However, all of them are very recent and several areas still need to be explored. In this project, it is intended to follow in the footsteps of Dominic S. Sebastian, Sonu K. Thomas, and T.M. Muruganandam in their study "Gas dynamic effects of shock interaction with the liquid jet in supersonic crossflow" [5]. Their study analyzes how, by incorporating a shock generator, the course of the supersonic waves produced by the high velocities can be altered so that they hit the fuel injection zone directly, promoting mixing and atomization, thus making the process more efficient.

The state of the art will be further developed in Chapter 2. where scramjet engines, supersonic waves and the problem of jet injection in supersonic flows is discussed.

1.3 MOTIVATION

This project aims to make breakthroughs and discoveries in supersonic speeds. Although there is still much to be known about scramjet technology, it can open countless doors for humans to achieve great advances in conventional aviation as it could be a way to complete enormous distances in just a few seconds. At the same time, it can bring about considerable progress by increasing the comfort of flights, decreasing their duration, and consequently reducing the current flight time between countries. This type of engine is also studied for military purposes such as the creation of hypersonic missiles.

Increasing combustion efficiency is a key step toward a better understanding of how these vehicles work. On the other hand, this project is also intended to guide future scientific research in aerodynamics, thermodynamics, or the use of new forms of energy.

1.4 PROJECT OBJECTIVES

This project aims to study the LJISC problem experimentally to better understand the combustion process in supersonic combustion stator jets. Thus, the objectives of this paper are to:

- Analyze the recent theoretical framework that examines past experiments and the respective conclusions reached in them. In addition, the behavior of supersonic waves is studied to carry out the relevant calculations.

- Explain the manufacture and design process of a supersonic wave generator (shock generator) capable of changing the path of the supersonic waves so that they hit directly against the fuel injection zone to enhance atomization.

- Finally, conclusions are drawn from the results that were obtained in the laboratory at the University of Minnesota. As it is intended to study the effect caused by the supersonic wave generator, a comparison is made between the fluid's behavior when the shock generator is added or removed.

It should be emphasized that this is a completely experimental study and that the expected results are, to some extent, new to everyone.

1.5 METHODOLOGY AND RESOURCES

In order to carry out this project, the laboratory facilities of the Department of Mechanical Engineering of the University of Minnesota, the Thomas E. Murphy Engine Research Laboratory, were used extensively. The facilities had all the necessary tools and equipment

necessary to carry out this experiment. In this laboratory, a mini wind tunnel was built to be able to extract the pertinent conclusions. Moreover, the relevant parts of the shock generator were sent to be manufactured at the University factory.

For the analysis of the results, tools such as MATLAB or ImageJ were used.

Schlieren photography was used to observe what was happening inside the wind tunnel through the variation in the density gradient since it would have been impossible to see with the naked eye. Thanks to Schlieren photography, it was possible to analyze the shock wave structure caused by the shock generator. Moreover, the use of backlight-illuminated imaging was necessary to analyze the resulting characteristics of the jet.

As for the theoretical part, for the research and information gathering, recent academic articles were used to extract pertinent conclusions. Specialized books on Fluid Mechanics were also used to develop and understand the formulas related to supersonic waves, which were necessary for the successful completion of the project.

Chapter 2. THEORETICAL FRAMEWORK

The objective of the study is to increase combustion efficiency of a scramjet, which occurs through increased atomization and mixing of the fuel with the air. This chapter is responsible for providing the reader with sufficient technical knowledge to understand the project in its entirety.

2.1 SCRAMJETS

From a Mach close to 2.5, engines with turbines and compressors lose efficiency due to the resulting drag of the mechanical structures [4]. This is no longer the case with ramjet engines. The invention of the ramjet is attributed to the Frenchman René Lorin in 1913 and stands out for its conceptual simplicity in achieving air compression by its internal geometry, which makes the use of mechanical structures unnecessary, generating thrust from the "ramming" effect of the air [10].

Ramjet (stator jet) engines operate by compressing the incoming air due to the high speed of the vehicle. In them, the inlet air is first decelerated to subsonic velocities. Then, fuel is injected and burnt to expand through a second throat to a thrust nozzle.

The problem that appears with this type of engines is that when speeds increase above Mach 5 it is difficult to reduce the inlet speed to achieve subsonic conditions. This produces significant shock losses in the inlet, in other words, a pressure loss due to the abrupt discontinuity in the flow field. In addition, it also leads to a considerable increase in flow temperatures in the combustor, resulting in chemical dissociation of molecules in the nozzle expansion leading to energy loss from the engine cycle [11].

On the other hand, the internal geometry of a scramjet is designed in such a way that although the air slows down inside the combustion chamber, it maintains its supersonic conditions throughout the engine. A scramjet, also known as a supersonic combustion ramjet, is at the

end of the day a variant of a ramjet airbreathing jet engine in which the flow is maintained supersonic throughout the engine.

For a better explanation, Figure 1 shows the differences in parts and flow rates of the ramjet and scramjet engines. The ramjet engine is shown on the left and the scramjet on the right.

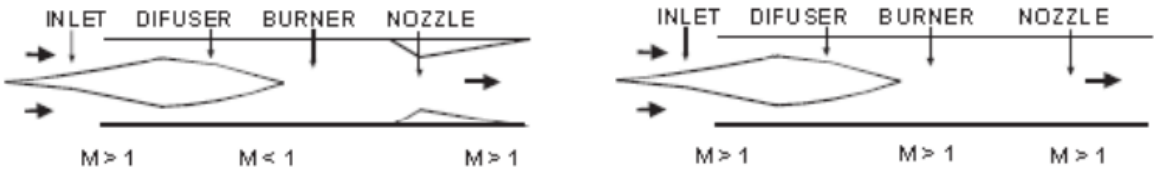

Figure 1. Comparison between a ramjet and a scramjet engine [10].

In both, the motor structure is divided into four parts. The first of these, the inlet, has the function of directing and compressing the air flow. Next, the diffuser is responsible for slowing the flow velocity before it enters the burner so that combustion can occur. Ramjet engines reduce the supersonic conditions to subsonic at this stage, while scramjet engines maintain the supersonic speeds. In the burner or combustor, the fuel is added, and the combustion gases are produced. These gases going through the nozzle at high velocities will be the responsible for generating thrust.

In ramjets the speed during combustion is reduced to subsonic conditions, so the nozzle is in charge of increasing the speed at which the combustion gases are expelled [12].

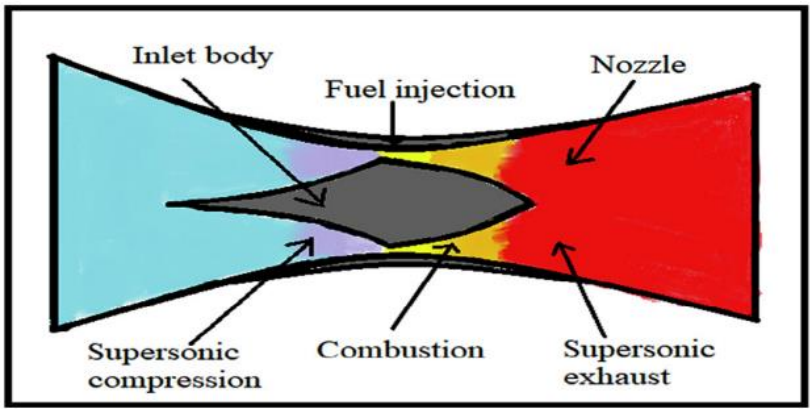

Figure 2. Internal operation of a scramjet [13] .

The advantage of the development of the scramjet over the ramjet is that it puts an end to the losses generated when the ramjet engine reaches high Mach numbers, and its diffuser is not efficient enough to slow down the flow velocity.

Moreover, for flights reaching Mach 6 and above the scramjets have a significant advantage over the rest of air-breathing engines and rocket propulsion engines. Figure 3 shows a comparison between the specific impulses of them.

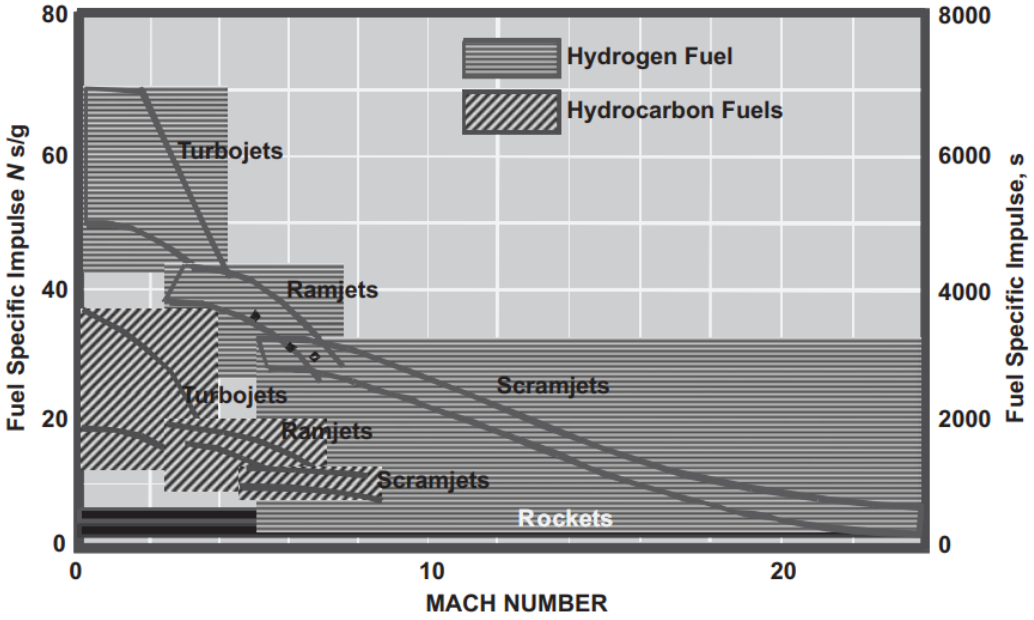

Figure 3. Specific impulse of different jet propulsion systems [10] .

Nevertheless, scramjets cannot work independently, since they cannot start running until they have achieved sufficient speed, which is why it needs first a different type of engine, such as a rocket engine, to gain the necessary velocity. The scramjet engine is ideal to come into operation at a second stage of the vehicle.

Scramjet technology did not begin to be studied in more depth until the mid-1950s. A 1958 study conducted by Weber and McKay at NASA's Lewis Research Centre concluded that the efficiencies of ramjet and scramjet engines increase between Mach 4 and 7, and that scramjets become more efficient at Mach 7 and above. Later, the work of Antonio Ferri contributed to a much better understanding of the problems involved in combustion at supersonic speeds [11].

For many years, scramjet engines were tested on the ground to study their behavior and many computer analysis and wind tunnel simulations were performed. It was not until 1991 when Russia achieved the first scramjet flight test [13]. In this test a Mach of 5.9 was reached. From 2000 onwards, much more research has been done into scramjet technology. In 2002 the scramjet combustion was tested through the HyShot program by the University of

Queensland in Australia, and it was in 2004 when the first flight scramjet-powered vehicle with full control surfaces was achieved with the X-43A. This was part of the of the NASA's Hyper-X program with a funding of approximately $230 million and eight years of duration [8], [14].

Scramjets can use different types of fuel, including liquid hydrocarbon fuels and gaseous hydrogen. Hydrogen has a wide flammability range and because of its short ignition delay, it can burn quickly and generate a large amount of thrust. Hydrogen is also safe and clean for the environment and can be produced from abundant sources. On the other hand, hydrocarbon fuels present much greater challenges compared to hydrogen fuel, mainly due to their longer ignition delay and the need for more advanced mixing techniques. Hydrocarbon-based fuels produce harmful pollutants such as carbon dioxide (CO_2), carbon monoxide (CO) or particulate residues during the combustion process [9]. Despite this, hydrocarbon fuels are beneficial because they can be stored in their liquid form without cryogenic systems.

Supersonic air propulsion systems depend on the quality of the fuel-air mixture which is the main challenge that scramjets face. This is because it is very difficult to achieve a proper mixture in the short residence time, which is only of about 1 millisecond, inside the combustion chamber due to the high velocities of the air [1]. Liquid-fueled scramjets face the problem of achieving proper fuel disaggregation at a molecular level and mixing within a fraction of a second [4]. Mixing along with the evaporation of the fuel needs to be achieved as quickly as possible for efficient combustion [2].

A variety of mechanisms are available to achieve fuel mixing; from simple diffusion, using parallel currents with different velocities, to mass mixture resulting from lines of crossed currents. The low efficiency of some of them compared to others is easy to clarify, as in the case of parallel currents, since this method requires long distances to complete the mixture at the molecular level, it would require the use of a long combustion chamber with disadvantages such as higher weight and more challenging heat maintenance at the walls.

One of the most promising fuel injection methods is LJISC -liquid jet in supersonic crossflow-.

2.2 THE LJISC PROBLEM

The first key step in increasing the combustion efficiency of a liquid-fueled scramjet is to achieve a good fuel-air mixture, and this depends essentially on the liquid fuel injection strategy and atomization [5] . Optimal fuel distribution and consequent atomization not only increases combustion effectiveness but can also reduce pollutant emissions from propulsion systems.

Transverse injection is a promising candidate for scramjet engines since it can achieve good mixing and fast atomization.

LJISC stands for - Liquid Jet in Supersonic Crossflow –. In the process, the jet is injected interacting with the supersonic crossflow and bends in the direction of the current due to the high aerodynamic force.

The process takes place in the combustion chamber where the air is slowed down but maintained at supersonic speeds. Figure 4 shows the process graphically.

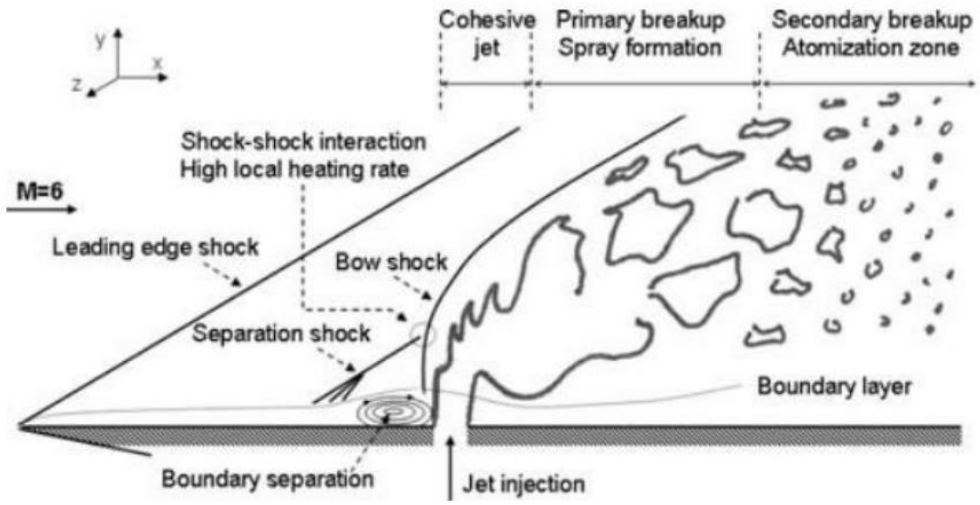

Figure 4. Diagram of the LJISC problem [3] .

The fuel shoots out vertically while the air flows horizontally to the wall. The blockage created by the liquid jet results in an upstream bow shock. This shock wave starts as a normal shock wave until it deforms into an oblique one. On this curve, all oblique shock waves can be observed together for a given Mach number. The bow shock wave originates in forming a curved shock wave detached from the nose of the jet. The zone between the bow shock wave and the jet is subsonic (Mach less than 1). This shock in turn interacts with the boundary layer and causes it to separate due to the adverse pressure gradient. Upon separation, a recirculation zone is formed along with a separation shock. As the jet turns in the direction of the airflow, it goes through three stages of breakup: a cohesive jet, primary breakup, and secondary breakup.

It is necessary to know the physics and characteristics of what happens in the LJISC problem to optimize the scramjet's performance. For this purpose, different experimental studies carried out by different authors have defined different parameters and common phenomena in the process in order to analyze the complexities of the problem. Among which the most important are:

- Jet-to-crossflow momentum flux ratio

The momentum flux ratio is vital when describing the interaction between the injected fluid jet and the crossflow. It is the most important variable in determining penetration height, hence its inclusion in the general equation. As expected, it has a positive correlation with penetration height. The momentum flux ratio is defined as such:

$$q = \frac{\rho_j u_j^2}{\rho_\infty u_\infty^2}$$

Where ρ is the density, u is the velocity and the subscripts j and ∞, refer to liquid and the air respectively.

- Penetration Height

Jet penetration height is one of the most studied parameters. It is the vertical distance from the injection orifice to the top of the jet spray plume. A higher penetration height is desired to achieve better combustion since better fuel dispersion is achieved. It is an important parameter for downstream mixing since it is related to the mass transport of liquid in the free airflow [4]. A generic equation of the penetration height is:

$$\frac{h}{d} = A(q)^B \left(\frac{x}{d}\right)^C (X)^D$$

Where h is the penetration height, x is the axial distance from the center of the injector orifice, d is the injector orifice diameter, q is the jet-to-crossflow momentum flux ratio, X is an additional parameter of interest, and A, B, C, and D are fit coefficients found through experimentation.

Height penetration can be studied using a variety of techniques such as shadowgraph, Schlieren, phase Doppler particle analysis (PDPA), or illuminated direct imaging.

- Droplet size

When a liquid is introduced into a high-speed gas flow, the relative motion between the gas and the liquid may cause the liquid to break down into droplets, this is called atomization.

These droplets are then entrained along the flow. The behavior of these droplets, their distribution and mainly their size may have significant effects on the efficiency of the combustion.

In particular, droplet size is important in determining the extent of jet atomization and breakup. Sauter mean diameter (SMD) is the measure that usually characterizes the average particle size for a polydisperse set of particles. In short, it compares the average diameter of a set of particles taking into consideration volume and surface area:

$$SMD = \frac{\int_0^\infty \frac{dn}{dd_p} d_p^3 \, dd_p}{\int_0^\infty \frac{dn}{dd_p} d_p^2 dd_p}$$

The integral of the numerator computes a weighted sum of the cubes of the particle diameters, and the integral of the denominator computes a weighted sum of the squares of the particle diameters.

Small droplet sizes take less time to evaporate and mix. Experimentally it was found that in an injector with a diameter of 1.3 mm, the Sauter mean diameter is of the order of 10 µm, which means that the larger the size of the injector, the larger the Sauter mean diameter is. This results in larger droplets [15]. The mean droplet size becomes smaller downstream during the secondary breakup.

- Surface waves

The creation of surface waves on the jet in the axial direction is mainly due to Rayleigh-Taylor and Kelvin-Helmholtz instabilities. The creation of the surface waves is key to understanding the primary breakup of the liquid.

The LJISC has been studied since the 1950s and many authors have drawn important conclusions experimentally. However, much remains to be known and much more experimentation is needed in many areas to better scramjet performance. That is why this study is carried out, to continue to learn more about this interaction.

This interaction is also studied in multiple engineering applications, such as in the aerospace industry for propulsion systems or in chemistry, to measure the behavior of the mixture in question.

2.3 SUPERSONIC WAVES BEHAVIOR

In this project, in order to achieve a better atomization a small wedge was incorporated in the upper part of the wind tunnel in order to alter the course of the supersonic waves so that they could hit the injected liquid. It is, therefore, inevitable to study the behavior of the supersonic waves.

Compressible flows are characterized mainly because density variations cannot be considered negligible and because they present a high energy flux. The most convenient way to determine whether a gas flow can be considered compressible is through the Mach number, M. Defined as the ratio between the local flow velocity (V) and the local speed of sound (a) (M = V / a) [6]. When the Mach number exceeds 0.3, the flow must be considered compressible.

Compressible flows can give rise to the formation of shock waves, which are fragile regions of space of 10^{-5} cm where the properties of the flow can change drastically [6]. In short, they are compressional processes where static pressure, density, temperature, and entropy increase discontinuously along the wave. Flow velocity and total pressure decrease, and the total enthalpy stays the same. An essential aspect of shock waves is the calculation of their geometry and strength. Thus, different types of waves such as oblique, normal, arc, etc. appear.

This project focuses on studying the creation of oblique shock waves. Such a wave is formed through a small wedge placed at the base of the upper wall. The angle of the wedge, the deflection angle (θ), must form a concave corner. If the corner were convex, instead of forming an oblique shock wave, an oblique expansion wave would be formed with the opposite effect, i.e., the pressure would be continuously decreasing along the wave-

expansion fan. Figure 5 shows the creation of an oblique shock wave in a supersonic flow over a corner with a deflection angle, θ. The shock wave characteristics are shown. A discontinuous static pressure, density, and temperature increase while the Mach number decreases.

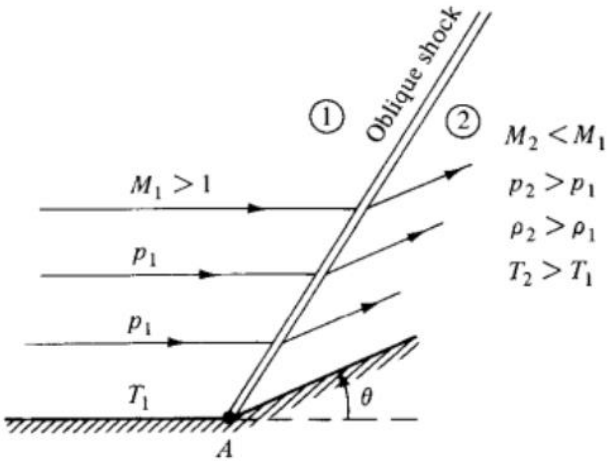

Figure 5. Supersonic flow over a corner [6] .

The reason why a corner/wedge generates an oblique supersonic wave is the propagation of air particles at the molecular level. The moving air particles bounce against the body, experiencing a change in their momentum and hitting the rest of the surrounding molecules, transmitting the information from one to the other. As the main flow is supersonic, the air molecules bouncing against the wedge do not have enough time to move against the upstream flow direction, so the particles coalesce to form a standing wave in front of the object.

For a better analysis of this project, it is crucial to define the relationship between the angles:

- The wave angle (β). It indicates the inclination of the shock wave concerning the central horizontal axis. In a particular case, normal shock waves present a wave angle of 90º.
- The deflection angle (θ). The angle of inclination of the wedge.

These two terms are related through the following formula (*M*- β- θ is related).

$$\tan\theta = 2\cot\beta\,\frac{M_1^2 sin^2\beta - 1}{M_1^2(\gamma + \cos 2\beta) + 2}$$

In it, the deflection angle remains a function of the M and β values.

Chapter 3. LITERATURE REVIEW

This section takes the reader on a review of some of the more prominent experiments that have been performed, along with their respective conclusions. It shows the reader that despite all the experiments that have been carried out, there are still many inconclusions and more research must be done. The most experimentally studied parameters are usually the penetration heights of the spray plumes, the sizes of the droplets formed and their velocity.

Along the years, several empirical correlations have been formulated to predict the penetration height of the spray plume.

In 2002, at the Air Force Research Laboratory, Lin *et al.* [16] studied the behavior of the liquid jet in a supersonic crossflow of Mach 1.94. The results were recorded by pulsed shadowgraph imaging and three types of liquids were used for testing: water, ethyl alcohol and a water/alcohol solution. For the experiments, injectors with different diameters of 0.5 mm, 1 mm and 2 mm were used and all measurements were performed at $x/d < 90$. In addition, different tests of $q < 20$ were compared in order to collect the data.

Shadowgraph imaging is a technique used to observe changes in the density of transparent fluids such as water or air. This technique visualizes density changes by showing shadows and regions of light and dark. The intensity of the shadow is proportional to the second derivative of the refractive index [17]. Basically, this means that the areas where the fluid density changes rapidly will produce darker shadows or brighter regions of light. Pulsed shadowgraph imaging is based on the shadowgraph imaging, but also adds the use of pulses of light, usually from a laser, to capture high-speed events that could not be captured with continuous light.

The correlations obtained in the experiment for the three liquids in a supersonic crossflow and using the least squares method are shown in Graph 1.

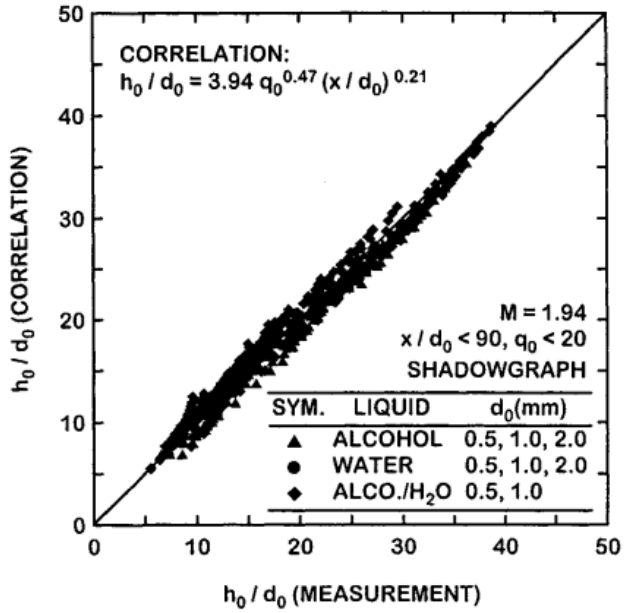

Graph 1. Penetration heights for pure liquid jets in supersonic crossflow [16] .

Two years later, Lin *et al.* [18] performed the same experiment with a crossflow with the same Mach number 1.94 and testing 0.5 mm and 1.0 mm diameter nozzles. Measurements were performed in a range of x/d = 25 - 200 and q = 2 - 15. This time, however, a two-component phase Doppler particle analyzer (PDPA) was used for imaging. This technique is used to measure the velocity and size of spherical particles in a more precise way.

PDPA system emits two laser beams that intersect at one point to form a sample volume. When the particle passes through the volume it interrupts the laser beams generating a scattered light signal forming a fringe interference pattern. As the droplet moves, the fringe pattern also does. It enters and leaves the sample volume at a specific frequency known as the Doppler difference frequency. The faster the droplet moves, the faster the fringe pattern will move and the higher the Doppler difference frequency will be. Thus, the velocity of the droplet can be determined. Size is determined by the spatial frequency of the fringe pattern. Larger diameter droplets have a lower spatial frequency and smaller droplets have a higher spatial frequency [19].

In the study, Lin *et al.* [18] also developed correlations for the calculation of the penetration height. The results are shown in Graph 2.

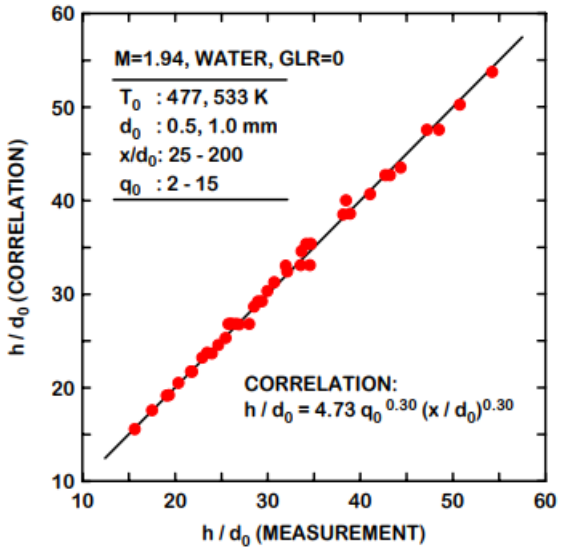

Graph 2. Penetration heights for pure liquid jets in supersonic crossflow [18] .

The penetration height predicted was higher than the one predicted in the previous experiment using shadowgraph imaging. This indicates that, depending on the measurement technique used, the results may vary. This is because the shadowgraph image method is only sensitive to the second derivative of the fluid density. Shadowgraph images are insensitive to low number density droplets with large diameters on the leeward surface of the jet, which PDPA is able to detect. On the other hand, PDPA measurements can be inaccurate in areas where the liquid has not completely atomized into droplets. This may happen with the measurement of ligaments, which are elongated liquid structures formed in the primary breakup and that have not yet broken into droplets. In other words, PDPA is a very good technique for the measurement of single spherical spots, but not for the overall structure of the spray plume [20].

So, it is important to note that for the same test conditions, the jet penetration height varies drastically depending on the diagnostic technique used. Moreover, correlations can also vary depending on where the jet boundary is set, i.e., how far the flow can penetrate a surrounding

medium. In the first experiment conducted by Lin *et al.* [16] the jet boundary was established as the point where the gray level of the average image had a transmittance of 90%. In other words, the jet boundary was defined by those points where the intensity of the laser light was reduced to 90% of its original value, since when the laser light passes through a jet, part of the light is absorbed and the intensity of the light decreases. In contrast, in the second experiment [18], measurements were stopped when the volumetric flow rate of liquid measured was less than 0.01 cc/s/cm^2. Shadowgraph, Schlieren and direct imaging can yield very different outcomes in terms of penetration due to the threshold selected for stablishing the boundaries of the jet.

More studies have been done on the correlation of penetration heights.

Ghenai *et al*. [20] developed correlations for penetration height for a Mach 1.5 also based on the least squares method and using laser illuminated direct imaging which is used especially when the fluid is dispersed. For this experiment, water and methanol were used as test liquids and tested at different momentum flux ratios as shown in Graph 3.

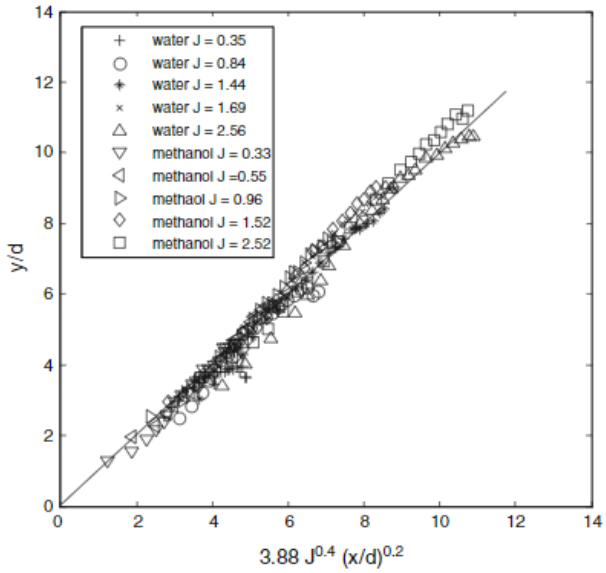

Graph 3. Penetration heights for pure liquid jets in supersonic crossflow [20] .

To bring a more recent correlation to the reader, in 2020, Sathiyamoorthy *et al.* [21] decided to study jet penetration through a tandem hole configuration. First, in order to compare the results, it was studied the penetration of a single-hole nozzle using shadowgraph imaging. The experiments were performed at Mach 1.9 and the diameter of the injector was 1 mm. Kerosene was used as the injection fluid. Kerosene is a type of liquid hydrocarbon commonly used as fuel. After testing different flux momentum ratios, the correlation shown in Graph 4 was reached.

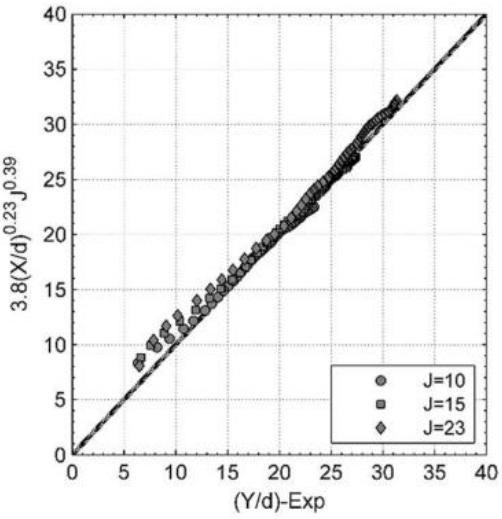

Graph 4. Penetration heights for pure liquid jets in supersonic crossflow [21] .

Table 1 shows the different correlations that have been mentioned above and their respective equations.

Study	Correlation
Lin *et al*. -2002-	$\frac{h}{d} = 3.94\, q^{0.47} \left(\frac{x}{d}\right)^{0.21}$
Lin *et at*. -2004-	$\frac{h}{d} = 4.73\, q^{0.30} \left(\frac{x}{d}\right)^{0.30}$
Ghenai *et al*. -2009-	$\frac{h}{d} = 3.88\, q^{0.40} \left(\frac{x}{d}\right)^{0.20}$
Sathiyamoorthy *et al*. -2020-	$\frac{h}{d} = 3.8\, q^{0.39} \left(\frac{x}{d}\right)^{0.23}$

Table 1. Correlations studied [16], [18], [20], [21].

The following graph shows a comparison of the four correlations with a momentum flux ratio of q=3 and q=5. Thus, it is demonstrated in a visual way how the different curves vary from each other and that there is still much to be known about the penetration height of the injected liquid. It is also observed that as q increases, the penetration height also does.

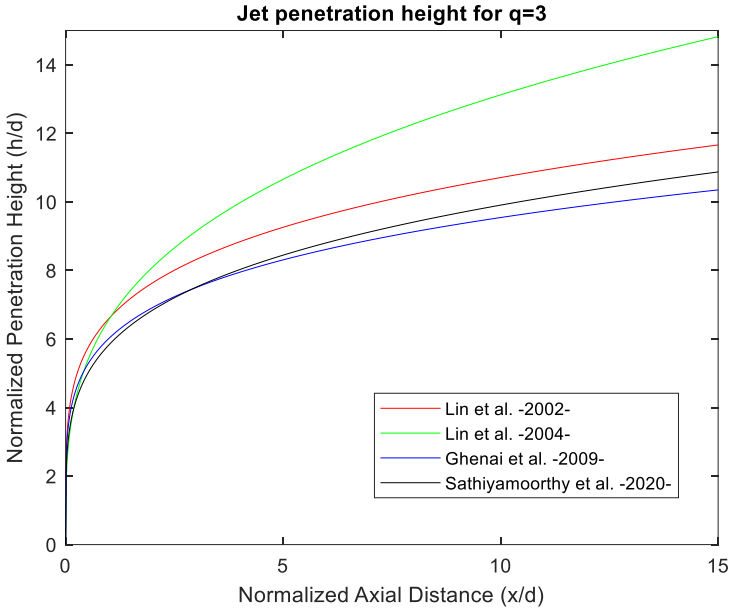

Graph 5. Comparison of the different correlations with q=3.

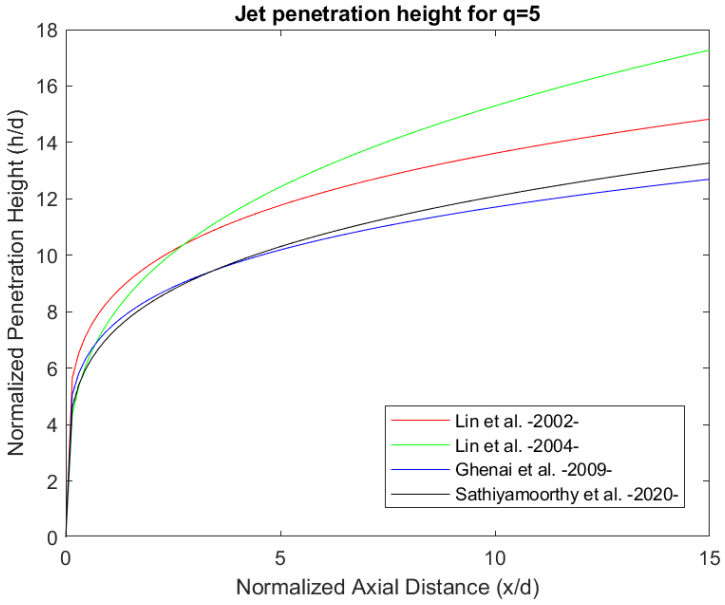

Graph 6. Comparison of the different correlations with q=5.

The other parameter that has been widely studied is the spatial variation of the droplet size in the spray plume. Small droplet size and low droplet velocity are desired as it contributes to better combustion [22].

Figure 6 , extracted from the study performed by Zhou Y *et al*. [23], shows the atomization process and the different zones of the droplet breakup.

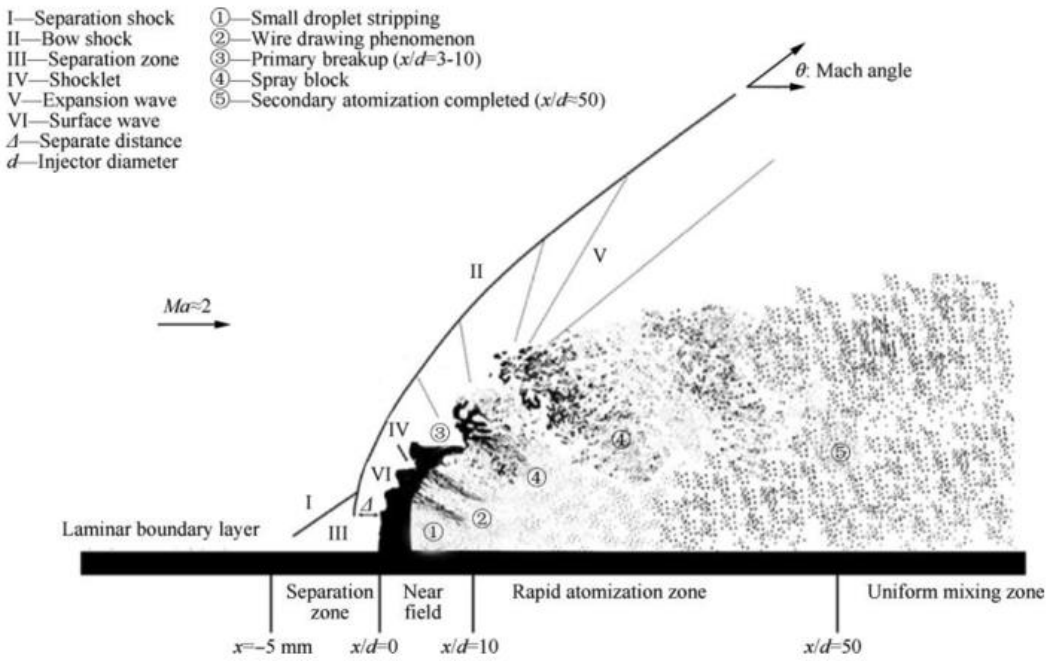

Figure 6. Atomization process of a LJISC [23].

When the liquid is injected, a series of instabilities occur, resulting in a surface wave. The axial surface wave with a high frequency and a large amplitude is a determining factor in the breakup of the liquid column.

Droplet formation is, partly, caused by Rayleigh-Taylor (R-T) and Kelvin-Helmholtz (K-H) instabilities. The growth of Rayleigh-Taylor unsteady waves is the primary cause of column breakup, while the development of Kelvin-Helmholtz unsteady waves is the main factor in droplet and surface breakup [23].

Kelvin-Helmholtz instability is a phenomenon that occurs at the interface between two materials with different densities when there is a tangential velocity gradient between them. It is characterized by the formation of waves or vortices at the interface due to the tendency to mix. On the other hand, Rayleigh-Taylor instability occurs at a density interface when

there is a normal acceleration acting on it. The last instability is more likely to occur for liquid jets due to significant density differences.

The primary breakup includes the rupture of the injected liquid column and is strongly related to the effects produced by the bow shock and the separation shock. Secondary breakup, on the other hand, is more related to the rupture of droplets [23].

Many studies have been conducted on the normalized water droplet size distribution.

As discussed on the previous chapter, Nejad *et al*. [24] conducted a study which concluded that for an orifice diameter on the order of 1.3 mm, in an air stream of Mach 3, the Sauter mean diameter (SMD) of the droplets is on the order of 10 μm. It was also determined that the droplet size decreases downstream, and that the diameter of the liquid injector plays an important role in droplet size and consequently in droplet atomization.

Since the use of the PDPA, much more information about this parameter has been collected.

In 2004, the experiments of Lin *et al*. [18] , using an injection diameter of 0.5 mm for a water jet, showed that the normalized distribution profiles for droplet size are *s*-shaped. Determining that this curve can be used for far-field structure shaping in the LJISC problem.

Lin *et al*. [18] studied positions at $x/d > 100$ and observed little change in the SMD profile at different locations which may indicate that liquid atomization was completed for $x/d=100$. It was determined that the smallest droplet sizes are reached where droplet velocities reach their maximum.

The *s*-shaped distribution is shown in Graph 7. It is important to note that to account for the different jet-to-crossflow momentum flux ratios, the cross-sectional distance from the injection wall, *y*, is normalized to the local penetration height, *h*.

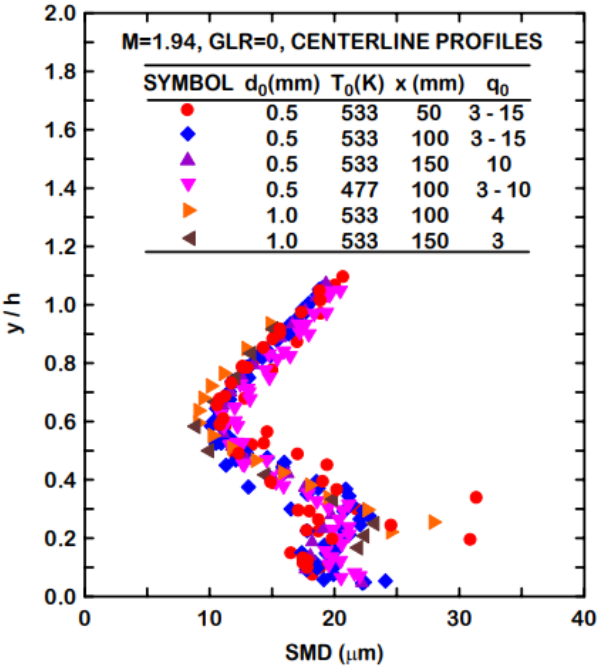

Graph 7. Normalized distribution profiles for SMD [18].

The largest droplet sizes appear at the top of the spray plume and at *y/h*=0.3, positions where the droplet velocity appears minimal. The *s*-shaped distribution can be due to the presence of the wind tunnel floor causing changes in aerodynamics and the occurrence of two inversion points one at *y/h*=0.3 and another at 0.6.

In a study carried out by Medipati *et al*. [25], PDIA (Particle/Droplet Image Analysis) was used as the measuring technique. For this technique, a short duration pulse laser is used to eliminate motion blur and a camera captures the results [26]. The SMD variation in the current direction had the same *s*-shape. The results shown in Graph 8 were at *x/d*=100. The results were measured at the centerline of the spray plume with *q*= 7 and Mach 2.5.

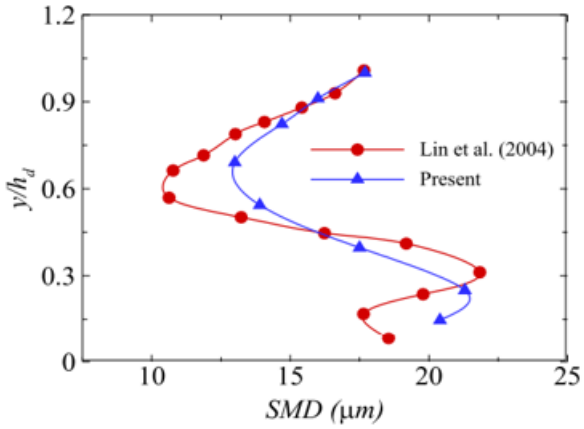

Graph 8. Comparison of normalized distribution profiles for SMD [25]

The strongest gas-liquid interaction process takes place in the windward region, the front region of the spray plume. There the normalized droplet deformation reaches its maximum value because the relative velocity of the gas and the liquid reaches its peak value. Along the test section, the relative velocity decreases and consequently the deformation of the droplets does [27]. Moreover, through Graph 7 and Graph 8, it is possible to observe how the liquid trailing phenomena is present in the process.

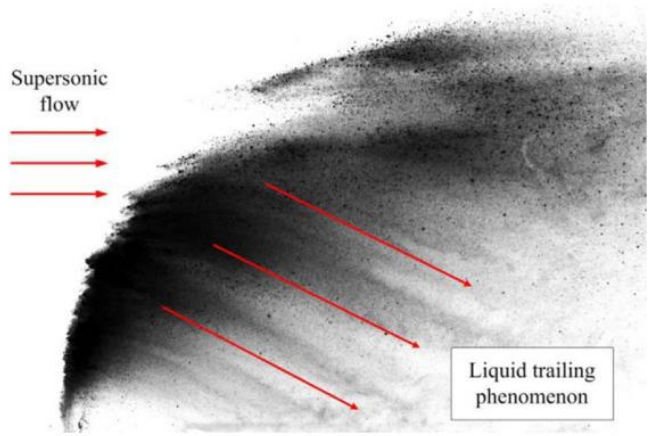

Image 1.Liquid trailing phenomenon [27].

Understanding this phenomenon is very important for the mixing process of liquid fuels in supersonic airflow. Figure 7 shows the droplets colored and sized according to their diameter.

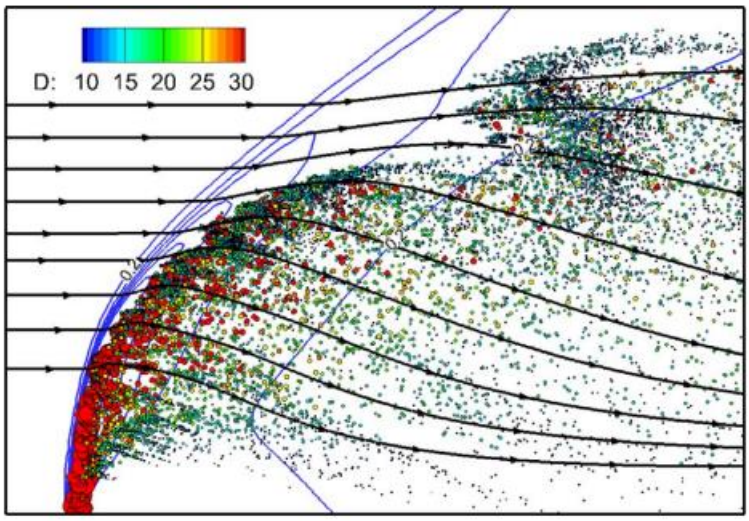

Figure 7. Droplets distribution on the liquid trailing phenomenon [27].

Due to the abrupt collision of the injected liquid with the supersonic air stream, the liquid ruptures rapidly into small droplets of different sizes, with the droplet groups concentrating in the frontal zone. The air stream flows downwards as a result of a pressure difference causing the droplets to move in the same direction. As the droplets are of different sizes,

they also acquire a different acceleration, so they are gradually molded into a series of liquid entrained structures along the local air flow. The larger droplets are distributed mainly in the outer region, while the smaller droplets are located in the lower part of the spray field [27].

In short, all the " child " droplets that are a consequence of an initial droplet are organized according to their size in a direction similar to the air flow.

Graphically, the process is explained in Figure 8.

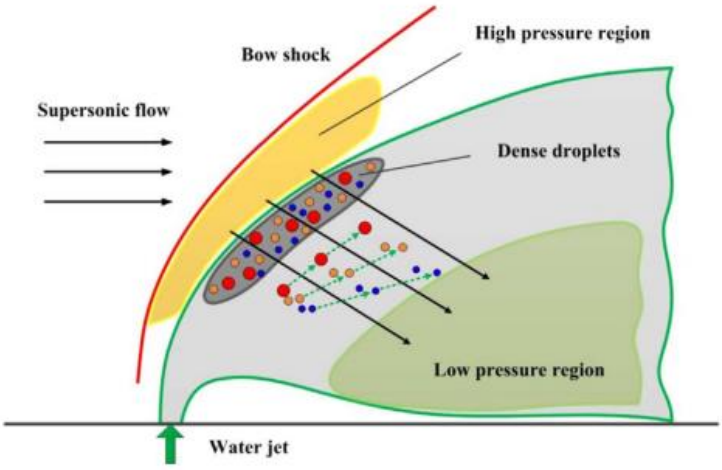

Figure 8. Scheme of the liquid trailing phenomenon [27].

It is the large droplets that experience the greatest breakup since the small droplets are in the center of the spray field where the shock and gas-liquid interaction is weaker. Consequently, in the downstream region, the relatively larger droplets are mainly located in the central region which is what causes the *s*-shaped distribution [27].

Nonetheless, other studies report different normalized droplet size distribution profiles. Li *et al.* [28] observed a *c*-shaped profile. The study was performed at different locations between x/d = 45-135. The experiments were conducted with different injection diameters between 0.7 mm and 1.4 mm and the airflow was Mach 2.85.

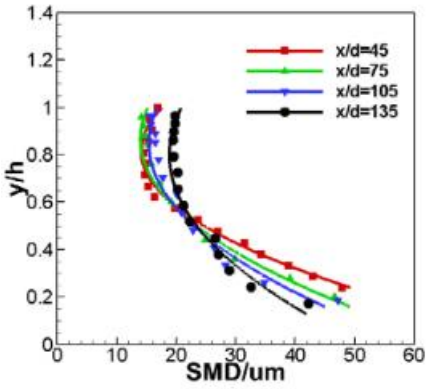

Graph 9. Normalized distribution profiles for SMD [28].

As the height of the spray plume increases, the droplet size becomes smaller. This may be due to a higher interaction between the supersonic air and liquid flow in the upper regions that does not meet the liquid jet column. The higher the *y/h*, the higher the droplet velocity.

The experiment showed that with the augment of the *x/d*, the SMD decreases downstream for $y/h < 0.5$. Although the inverse trend is observed when $y/h > 0.5$, making the SMD larger downstream. Similar profiles were obtained with the different injection diameters used.

This also shows the inconclusions that appear in this study area.

However, what is really of interest in this project is how to achieve a higher liquid penetration height to make the atomization process more efficient. For this purpose, numerous experiments have been conducted in the past to test the effects on the penetration height by varying the injection angle of the liquid or the consequences it has if the injected liquid is aerated.

The technique of barbotage or the aerated liquid jet, where a small amount of gas is added to the liquid fuel, can be used to accelerate atomization and the mixing process between air and fuel [29]. When the amount of aeration gas increases, the liquid film becomes thinner in the coannular flow. This causes the gas/liquid velocity ratio to increase at the nozzle outlet, i.e., the gas is moving faster through the system compared to the liquid. In addition, the momentum flux at the outlet also increases [20].

Sallam *et al*. [30] studied the atomization process of aerated liquid jets in supersonic Mach 2 transverse flows. Digital holography, which is a technique that uses light interference to create 3D images, was used in the region near the injector at $x/d < 50$. In the tests, they used different levels of GLR. It was concluded that the thinning of the liquid film leads to a further reduction in water droplet size. As for the penetration height, an increase in the gas-to-liquid ratio (GLR) means an increase in the spray plume formed. The GLR is one of the most commonly used parameters to measure the characteristics of an aerated liquid jet.

$$GLR = \frac{\rho_g Q_l}{\rho_l Q_l}$$

where Q is the volume flow rate and the subscripts g and l, refer to gas and liquid respectively.

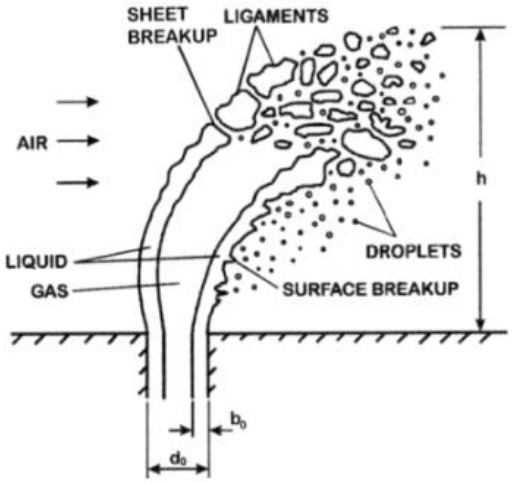

Figure 9. Break up process in an aerated liquid jet in supersonic crossflow [30].

Ghenai *et al.* [2] also experimentally studied the aeration of the liquid jet. Nitrogen was used as the gas, and it was demonstrated that aeration of the liquid positively affected the jet penetration height due to the increase of the jet-to-crossflow momentum flux ratio. Jet penetration increased as GLR increased.

Nevertheless, this study focuses on how the addition of a shock generator may increase the penetration height. As it will be discussed on the following chapter, the results and

conclusions drawn from other experiments seem inconclusive and there is still much to be investigated since numerous factors may come into play such as the design of the shock generator or the point of impact of the incident wave created by the shock generator.

Chapter 4. EXPERIMENTAL DESIGN

The experiments were carried out at the Thomas E. Murphy Engine Research Laboratory at the University of Minnesota. This section intends to explain the experiment that has been used as the model to be followed and the tools used to carry out the experiment.

4.1 STARTING POINT

The study conducted by Sebastian *et al*. [5] and published in 2022 was used as the model experiment. This is because, although the experiment requires further study, the results obtained were promising and few research has yet been done on the use of a wedge in the atomization process.

The experiment was conducted at the Gas Dynamics Laboratory at the National Centre for Combustion Research and Development of the Indian Institute of Technology Madras. In the wind tunnel, Mach 2 was set, and the injector diameter was of 1mm. In addition, Schlieren imaging was used for flow field analysis. A schematic of the test section is shown in Figure 10.

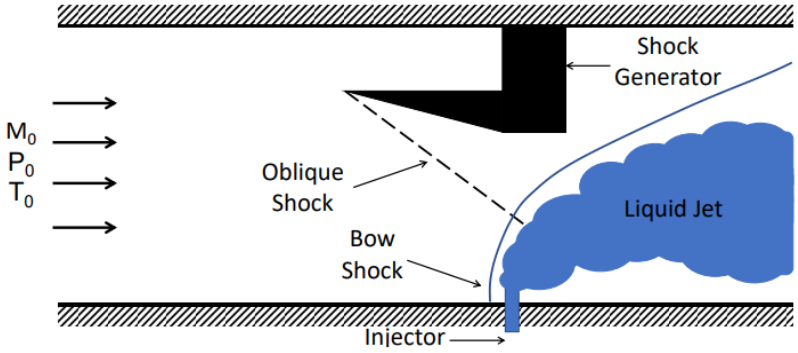

Figure 10. Test section [5].

A wedge was located at the top of the test section and it was responsible for producing an oblique shock wave that collided and interacted with the injected liquid jet. The oblique

shock generated by the wedge was an incident shock (IS) wave and was generated by the starting point of the wedge.

In the experiment, the wedge was inclined 10° with respect to the upper wall and the length of the wedge was varied to analyze different cases and interactions between the liquid and the supersonic air flow. Water at different pressures was used as the injected liquid for the study.

The impact point of the incident shock varied as a function of the wedge angle. Assuming an inviscid flow, without considering the effects of the shock boundary layer, the point of impact was called as the theoretical shock impinging point (TSIP) and it was denoted as L_0 when the wedge was located 10 mm below the injector nozzle and L_{20} when the wedge was 20 mm below the initial position. With a higher wedge angle, the wave hit the strong bow shock zone closer to the injector zone.

When the wedge was located in the initial position the generated supersonic wave impacted directly against the strong zone of the bow shock which caused the wave to be reflected back. The bow shock merged with reflected shock (BR). Moreover, a separation shock (SS) was generated before the liquid jet (LJ) due to the interaction between the boundary layer and the bow shock. The iteration between the bow shock and separation shock was very important since it affected the effective momentum flux ratio near the injector, which influenced the formation of surface waves upstream of the liquid injection, which was responsible for the primary breakup of the jet. It also influenced the penetration height [5].

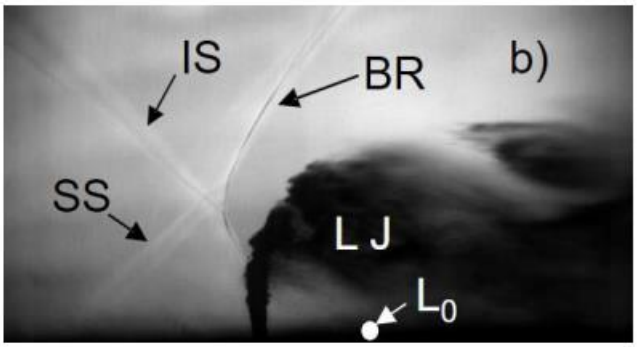

Image 2. Interaction with the jet at the strong part of the bow shock [5].

However, when the incident shock hit a point farther away, it did not hit the strong part of the bow shock. As a result, it was generated a rebound wave, also known as transmitted shock (TS). In the experiment, this wave was much weaker and refracted through the multiphase flow. According to the study [5], it was not known what happened when this shock wave was refracted, nor what characteristics it had.

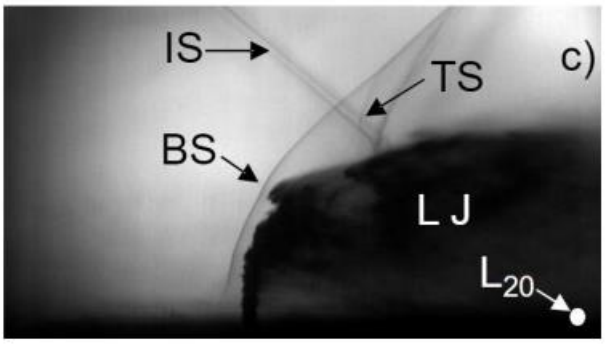

Image 3. Interaction with the jet at the weak part of the bow shock [5].

A study was carried out on the penetration height of the liquid injected at 6 bar.

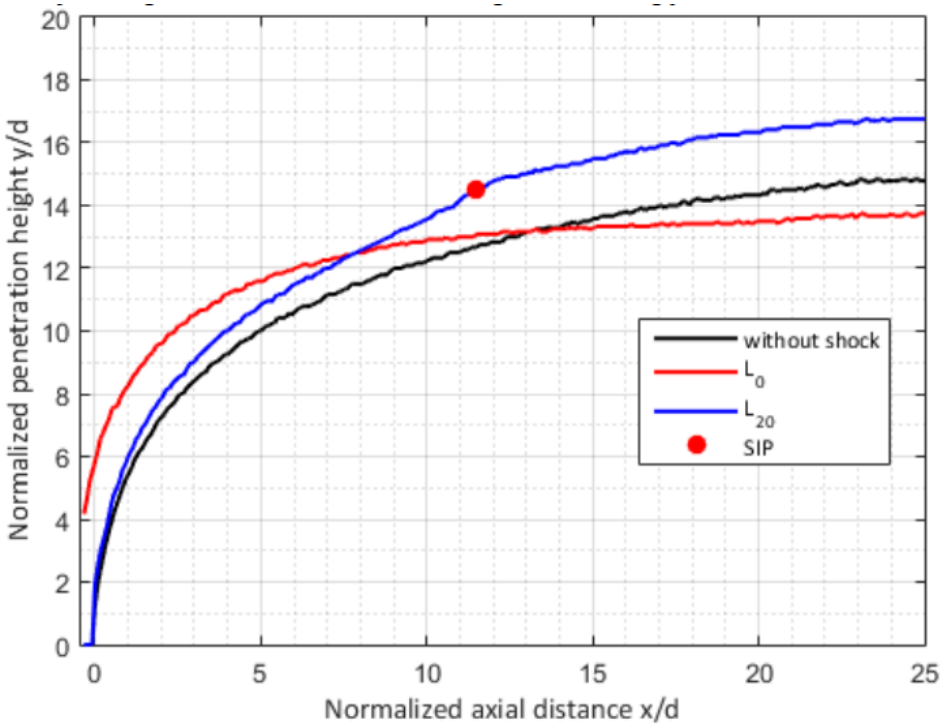

Graph 10. Height penetration curves [5].

It was observed that the base case had the lowest penetration height. With the addition of the shock generator, in any of its positions, the penetration height increased. The maximum penetration height was reached in the case where the wedge was positioned at the initial location although the curve then decreased with respect to the rest. This could be explained by the fact that the incidence shock wave was acting on the strong part of the bow shock which was likely to increase the subsonic region created between the bow shock and the jet. This allowed the liquid jet to penetrate further into the windward side since the aerodynamic forces acting on it decreased. The rapid descent that appeared later in the curve may have been because the oblique shock wave was pushing the air downward, which caused the fluid jet to bend downward as well. The figure also shows the shock intersecting point (SIP), which is the point where the incident shock hit the weak part of the bow shock and that was formed when the wedge was located 20 mm away from the initial position [5].

Few experiments have yet been conducted on the benefits that a generator shock can bring to the penetration height. However, the few that have already been performed show some inconclusiveness and, in the words of Sebastian *et al.* [5] "further investigation is needed".

Zhao *et al.* [31] conducted an experiment in an expansion wind tunnel showing that the penetration of the spray is reduced with the interaction of the generated supersonic waves. Three different zones were identified in the atomization process. The first zone, where the liquid was injected, was where the first breakup of the jet into smaller droplets occurred. In the second zone, an expansion wave accelerated the flow upwards as a result of the volume expansion. Finally, the third zone is where the interaction between the incident shock wave and a reflected oblique shock wave occurred (conditions similar to those of interest in this study). However, in this experiment, the direct impact of the incident shock wave against the jet was not studied.

Erdem *et al.* [32] carried out an experiment where the effect of an incident wave on a liquid jet was evaluated. In the experiment, the relative position of the incident shock wave with respect to the jet was varied to see the interaction at different locations. Four positions were studied: x/d=-5,0,5 and 10.

For the first location the jet penetration is considerably reduced due to the early interaction between the boundary layer and the incident shock wave. However, for the other three, similar jet behavior is observed when the same experiment is performed in the absence of the shock generator.

The incident shock wave interacted with the bow shock, bending the bow shock in the direction of the main flow in the cases where x/d =5 and 10. However, downstream of the intersection between the incident shock and the bow shock a pressure change was also observed which could have affected the jet dynamics and penetration capability. An increase in pressure behind the jet could slow down and decrease penetration, while a decrease could cause the jet to advance farther.

4.2 WIND TUNNEL

A mini wind tunnel was built in the laboratory of the University of Minnesota in order to realize the experiments and study the results. For its better understanding, the wind tunnel can be divided into two parts. The first, the air system, through which the desired Mach number was achieved. And the second, the water system, in charge of injecting the water into the supersonic flow.

4.2.1 AIR SYSTEM

Mach values between 1 - 3.5 could be achieved in the facilities. The wind tunnel utilized an Amrad nozzle which had a variable throat. In this study, the nozzle was adjusted to achieve a Mach number close to 2. The test section had dimensions of 6.35 mm wide, 9.83 mm high, and a length of 90.45 mm. It is coated on both sides with transparent UV-grade acrylic panels in order to perform the imaging study. In addition, a plenum chamber was used to distribute the air as evenly as possible before entering the throat and the test section.

Inside the plenum chamber there were screens or grids arranged in such a way that the air passed through them. These screens acted as an air distributor, breaking up the high velocity air flow coming from the inlet tube and distributing it more evenly before passing through the variable throat and entering the test section.

Compressed dry air was stored in the tanks, reaching up to 2500 psi. It was the only time when the pressure, at which the experiment was going to be carried out, was regulated. It must be taken into account that if the pressure was increased too much, it could lead to the throat's deformation.

Three pressure transducers were part of the wind tunnel facility and were used to gather pressure data. One was located in the plenum chamber, another in the test section base, and the last was used to measure the water flow pressure.

Figure 11 shows a schematic diagram of the different parts that composed the air system of the wind tunnel.

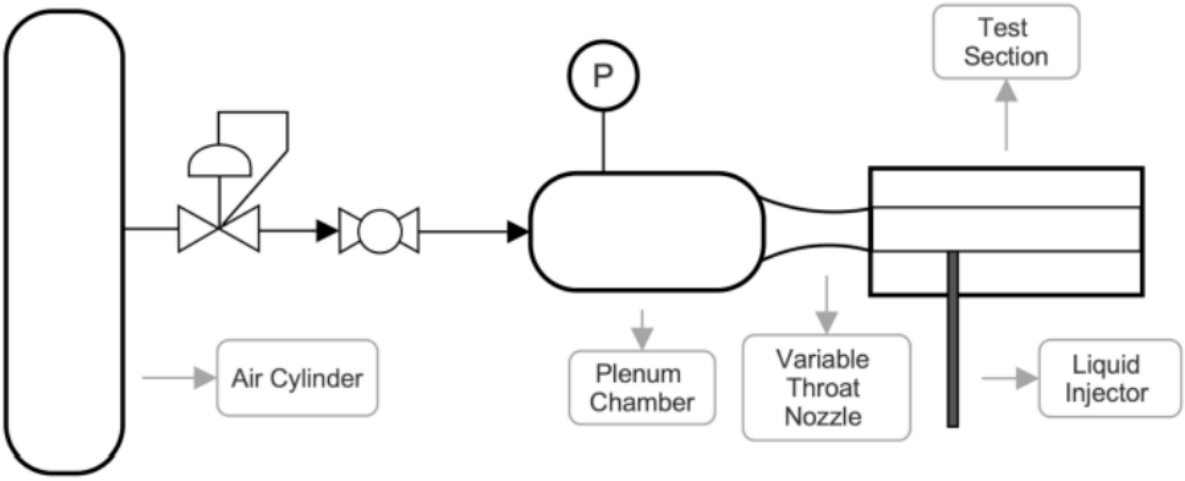

Figure 11. Diagram of the UMN wind tunnel facility.

4.2.2 WATER SYSTEM

The test section had a hole at the bottom through which the liquid was injected. The hole was 52.85 mm away from the end of the test section.

The liquid was stored in a reservoir which was pressurized, through an air intake, to 40 psi. An orifice flow control valve controlled the flow rate. The system was connected to the injection zone via tubes.

Figure 12 shows a schematic diagram of the different parts that composed the water system of the wind tunnel.

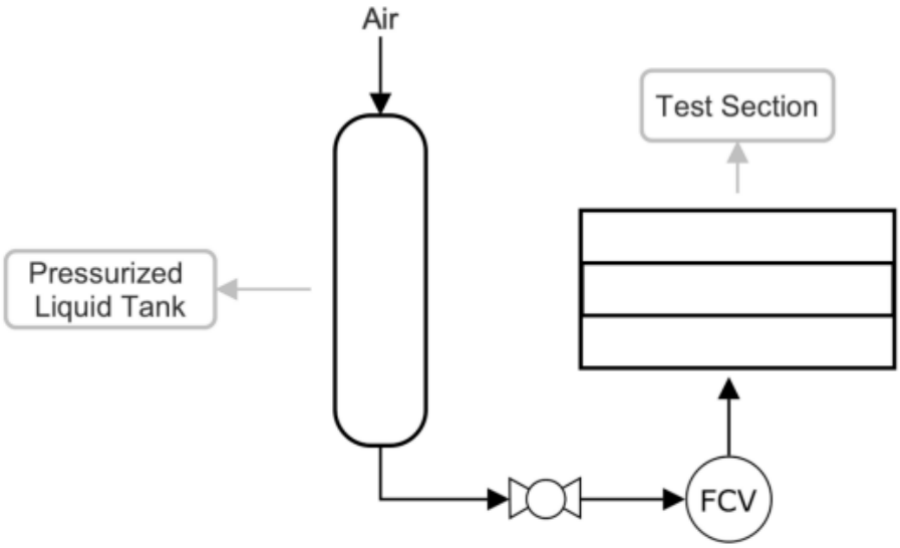

Figure 12. Diagram of the external liquid injection system.

4.3 SHOCK GENERATOR DESIGN

The study section was designed and modified using SolidWorks tooling. The model of wedge used by Sebastian *et al.* [5] was decided not to be used because of the possible back pressure generated at the top of the wedge. Instead, it was decided to use a wedge whose base was directly attached to the upper wall. Equation mentioned in Chapter 2 was used in order to see what the theoretically optimal model would be. The parameters used were Mach 2 and γ =1.4. Given the wind tunnel measurements, it was obtained that a wedge of 19 º had to be produced so that the generated shock wave would impact directly on the point of interest. The outline of what was attempted to be studied is shown in Figure 13.

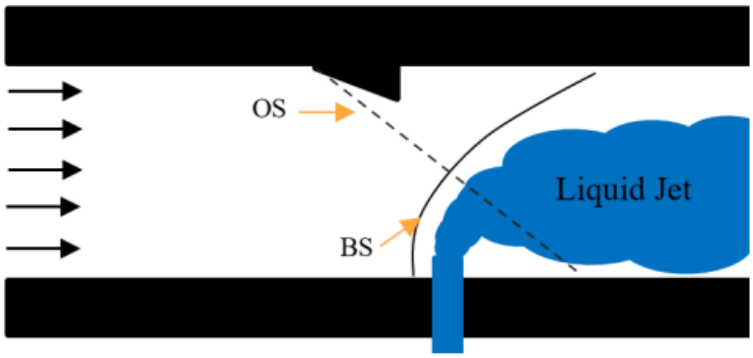

Figure 13. Diagram of the test section.

4.4 METHODOLOGY USED

In this laboratory, in order to study the behavior of the liquid in the supersonic flow it was used Schlieren imaging and direct imaging techniques.

4.4.1 SCHLIEREN IMAGING

Schlieren imaging is used in compressible fluids since the rays bend through a medium with a density gradient.

The principle that is used in this method is the principle of refraction. The refractive index (*n*) of a medium indicates how much the speed of light is reduced in that medium. When a ray of light passes perpendicularly through an area with a change in the refractive index, the speed of light will be slower but will still travel in the same direction. However, when the light ray passes obliquely through the refractive index, the ray will change its direction and tend to travel towards regions with a higher *n* [33].

What is analyzed in Schlieren's imaging is similar. When parallel light rays (without crossing each other) pass through a density gradient, they experience changes in the refractive index, which causes the light rays to deflect or refract. Figure 14 shows how light rays refract as a function of density gradients. Changes in the direction of light are perceived as changes in light and shadow.

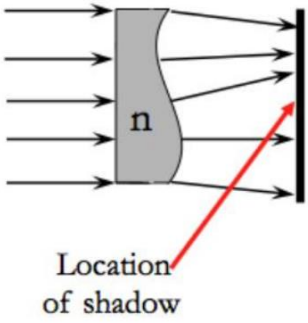

Figure 14. Location of shadow [33].

A light source was used to implement Schlieren imaging, which was regulated using lenses. The light converged at a single point through a slit to the first parabolic mirror. This collimating lens converted the divergent light from the light source into a parallel beam of light that passed through the test section, where the fluid, whose density gradient was to be studied, was located until it reached the second parabolic mirror or focusing mirror. The primary function of this lens was to concentrate all the rays at a focal point where a knife edge was placed to block the reflected light partially. The light that was blocked by the knife edge is called "cutoff". Blocking this light created a higher contrast in the resulting image that was recorded through a camera. In this case, an IX 727 high-speed camera was used.

A diagram of the process is shown in Figure 15.

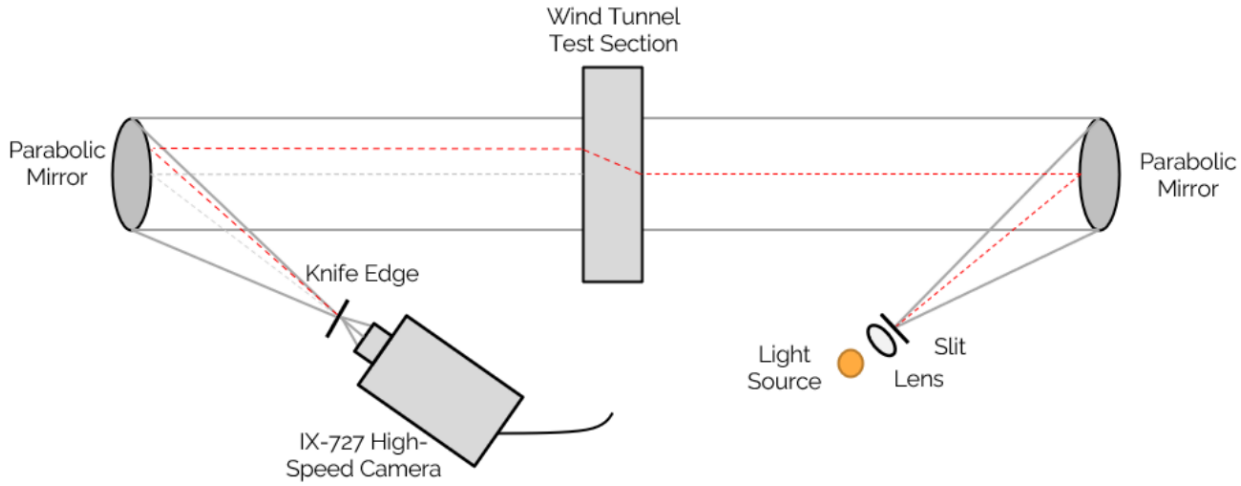

Figure 15. Diagram of Schlieren imaging.

4.4.2 DIRECT IMAGING

One of the problems that arose when experimenting was that when the wedge was added as a shock generator, the recorded images were utterly dark after a short time.

After a few milliseconds, the liquid started to flow upstream against the flow direction. This was due to the rapid separation of the boundary layer. The separation of the boundary layer was caused by the adverse pressure gradient. The separation of the boundary layer created a recirculation zone which caused water from the jet to move upstream since the wind tunnel was narrow. It was then, when some of the water droplets sticked to the acrylic and eventually found a way back into a region where the velocity of the air was downstream.

The water molecules that sticked to the acrylic windows made it challenging to study what was going inside the wind tunnel since they darkened the image due to differences in pressure gradients.

The process occurred as follows:

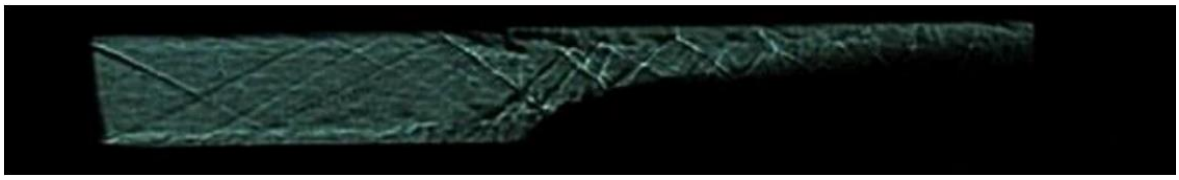

Image 4. Start of the liquid injection.

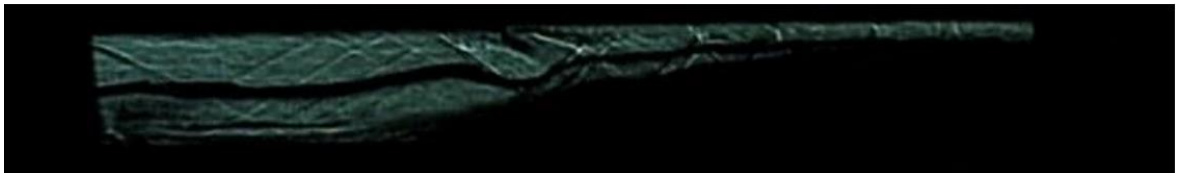

Image 5. Water flowing upstream.

Image 6. Image turns completely black.

Image 7 shows the boundary layer separation:

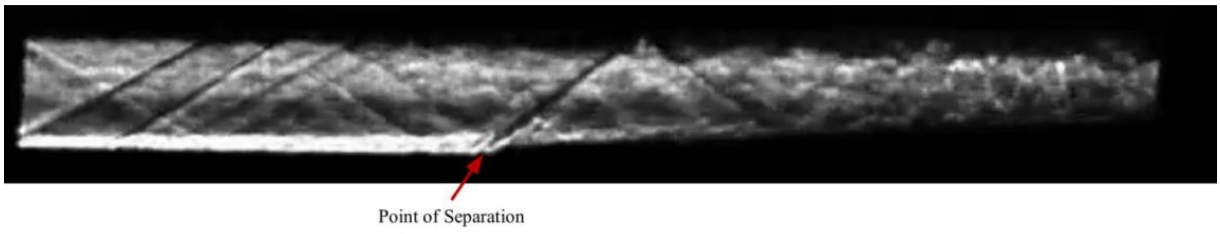

Image 7. Boundary layer separation.

For this reason, direct imaging was performed using a white LED panel as a backlight. In the studied images, a darker pixel indicates that the jet is still in the liquid phase, while lighter pixels just indicate that there is less of water liquid phase present.

For further study of the data, ImageJ and MATLAB were used to analyze the videos obtained using the above methods.

4.5 EXPERIMENT EXECUTION

The experiments were run at a tank pressure of 1900 psi. The pressure in the water injector was set to 40 psi. The compressed air tanks had an approximate duration of about 3-5 tests.

The DAQ (data acquisition system) to collect the information had a data collection frequency of 500 Hz, which means that information was collected every 1/500 s.

The first experiment's where Schlieren imaging was used and the supersonic waves' behavior was studied, were recorded at 200,000 fps, and the shooter speed was of 2 µsec. On the other hand, the second experiment in where direct imaging was used, the videos were recorded at 40,000 fps, and the shooter speed was of 24.46 µsec.

Finally, it is essential to note that only water injection was used in this project. The diameter of the injector was of 1mm, and the flow rate was of 530 cm^3/min. The Mach number achieved was approximately 2, the total temperature of the room was of 298K, and the stagnation pressure measured in the plenum chamber was approximately 85psi or 6894.76 Pa throughout the experiment. The momentum flux ratio was q = 0.3 and it was calculated using the isentropic relations.

$$\frac{T}{T_0} = \frac{1}{1 + \frac{\gamma - 1}{2} * M^2}$$

$$\frac{p}{p_0} = \left(\frac{T}{T_0}\right)^{\frac{\gamma}{\gamma - 1}}$$

Where p_0 is the stagnation or total pressure, T_0 is the stagnation temperature and p *and* T are the static pressure and temperature, respectively.

And other equations such as the ideal gas equation or the speed of sound equation.

$$\rho_\infty = \frac{p}{RT}$$

Where R is the universal gas constant.

$$a = \sqrt{\frac{\gamma P}{\rho_\infty}}$$

$$u_\infty = a * M$$

This way the values of $\rho_\infty \; and \; u_\infty$ are obtained since $\rho_j \; and \; u_j$ are data:

$$q = \frac{\rho_j u_j^2}{\rho_\infty u_\infty^2}$$

In Appendix I. Wind tunnel Facilities. there are shown more images of the University laboratory.

Chapter 5. ANALYSIS OF RESULTS

The purpose of this chapter is to present the reader the results obtained in the laboratory. Throughout the chapter, different images will be presented. They show the average image of the video recorded for the different cases after averaging over 10000 frames. Thanks to the use of MATLAB, it was manually ensured that only the test section was displayed in order to calculate the penetration height as accurately as possible.

5.1 SHOCK WAVES ANALYSIS

For this first experiment, Schlieren technique was used in order to visualize the supersonic waves.

The oblique shock waves that hit a solid surface are reflected on that surface, maintaining the geometry of the initial wave. When an oblique shock wave appears, it does not disappear when it rebounds against the wall but gives rise to the so-called reflected shock waves and follows the same wave angle as the initial supersonic wave. However, they are much less intense and strong. This is demonstrated on Image 8 where the supersonic waves that were created are marked with red arrows and their respective reflected shock waves can be observed.

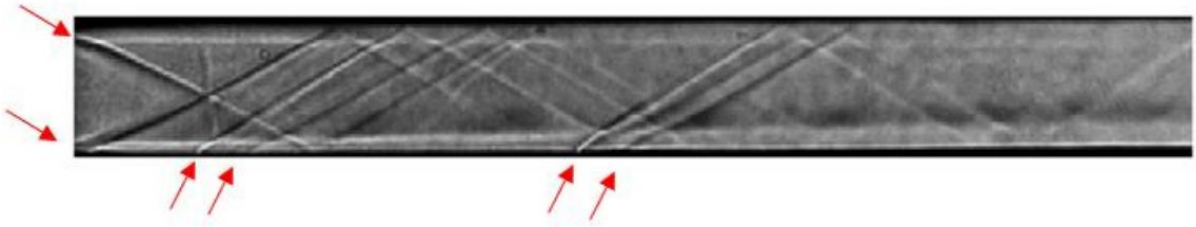

Image 8. Baseline.

The shock waves generated are due to small disturbances that appear in the wind tunnel. The first two supersonic waves were generated by the small gap at the entrance of the wind

tunnel. This was due to the fact that there was an edge at the boundary of the test section and the Amrad nozzle which caused these waves. A little further on, in the base of the test section, two new supersonic waves were generated. These were created by the small hole where the pressure transducer was located, which was in charge of collecting the information in the test section. The last two supersonic waves were created by the hole through which the liquid was injected.

The image shows how the first supersonic waves were very intense, however, as they bounce against the walls, they lost intensity that is the reason why the lines are becoming weaker and less visible each time they bounce off.

In the following images, the shock generator was added. These images show the different shock waves the wedge produced depending on its angle. The same shock waves as those produced in the baseline case appeared, plus the new ones that were formed due to the addition of the shock generator at the top of the wind tunnel.

Image 9. Wedge of 12º.

Image 10. Wedge of 15º.

Image 11. Wedge of 19º.

According to the theoretical results, the optimal case was presented for the 19º wedge since the shock wave generated would impact in the zone of interest. Throughout the process, several unforeseen events arose that were not expected. First, the small section of the tunnel meant that when any disturbance was added, the flow became very unstable. The images show that when any wedge was added, a strong oblique shock wave was formed from the back of it. This may be due to the separation of the boundary layer and the big turbulences created in the area due to the rapid compression and expansion of the flow due to the small dimensions of the wind tunnel.

However, the one that was of interest was the shock wave created at the front since it would be the one to hit the bow shock at the strongest point. But when the 19 º was added, it showed practically non-existent due to the instabilities of the system.

In the case of the 15º wedge, a well-defined supersonic wave appeared in front of the body. However, it was more similar to a detached shock. The formation of detached shock waves are due to the inability of the flow to conform to the geometry of the body it encounters. This is directly related to the angle at which the supersonic flow meets. A detached shock wave

forms if the wedge angle is greater than the maximum possible angle for an oblique shock wave to form.

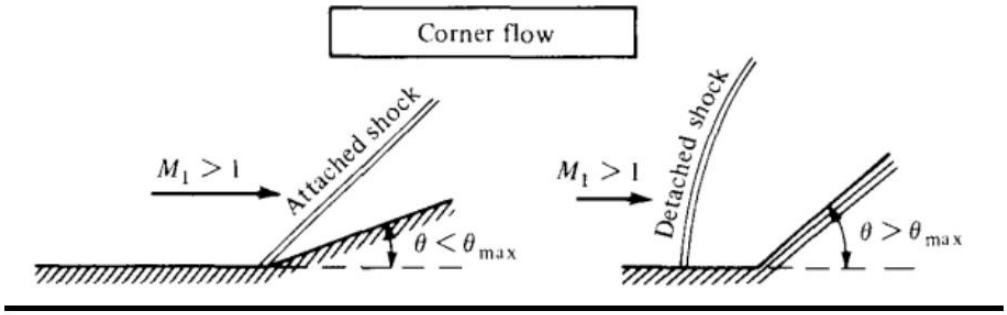

Figure 16. Diagram of detached shock [6].

Thanks to ImageJ, it was possible to make a comparative table between the theoretical calculations and the results obtained in reality. It should be noted that the theoretical results were made with Mach 2, due to the results obtained in the first instance in the wind tunnel. However, in the wind tunnel, an exact Mach 2 was not always achieved, but close to it. This may have occurred due to the loss of pressure in the compressed air tanks each time an experiment was run.

	Wave Angle	
Wedge Angle	**Theoretical results**	**ImageJ**
12º	41.576º	38º
15º	45.345º	32º
19º	51.503º	36º

Table 2. Results.

The theoretical results were very different from the practical ones. The results may seem far-fetched. However, to achieve a 38º angle with a 12º wedge under the specified conditions (γ=1.4), a Mach 2.192 must occur. This shows the considerable variations that appear in the

face of small changes in Mach number. A small variation in the Mach number has consequences on the shock angle that the wedge creates.

Therefore, for the second experiment, the smaller size wedge was chosen, the 12º wedge, which could present more coherent results.

5.2 ANALYSIS OF THE PENETRATION HEIGHT

Once the behavior of the supersonic waves had been verified, a study of the penetration height was carried out. The penetration height was calculated on the average image achieved after averaging over 10000 frames of the video recorded.

Image 12 shows three snapshots at different times of the atomization process. Image 13, on the other hand, shows the average image.

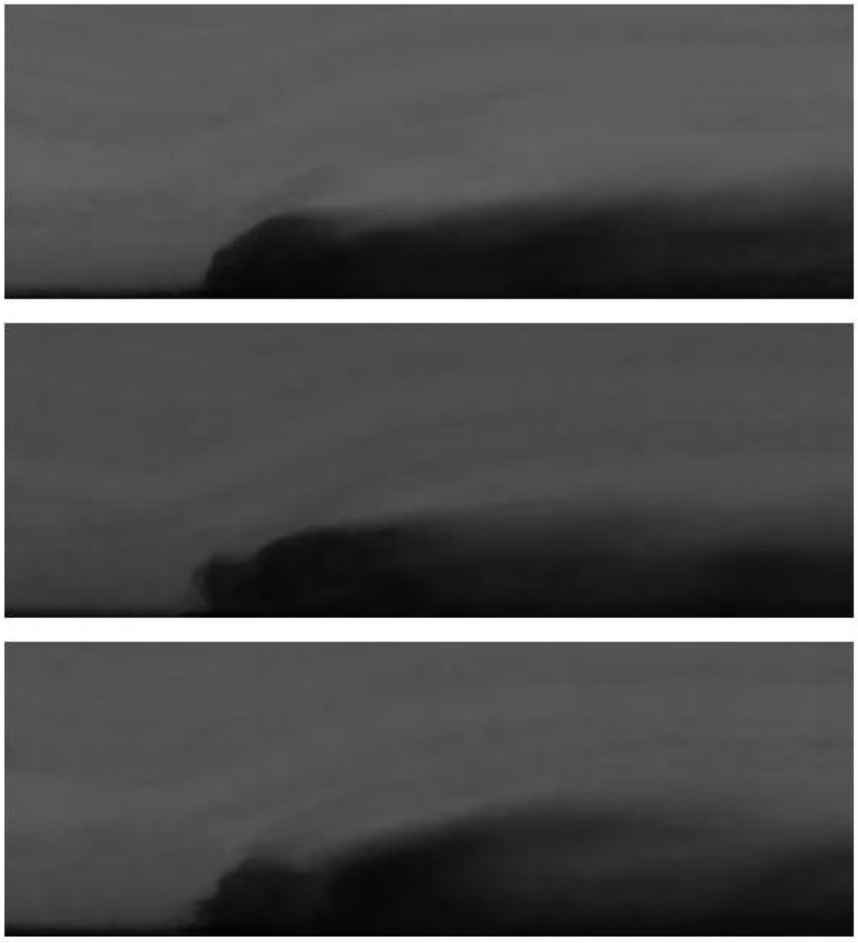

Image 12. Instant images.

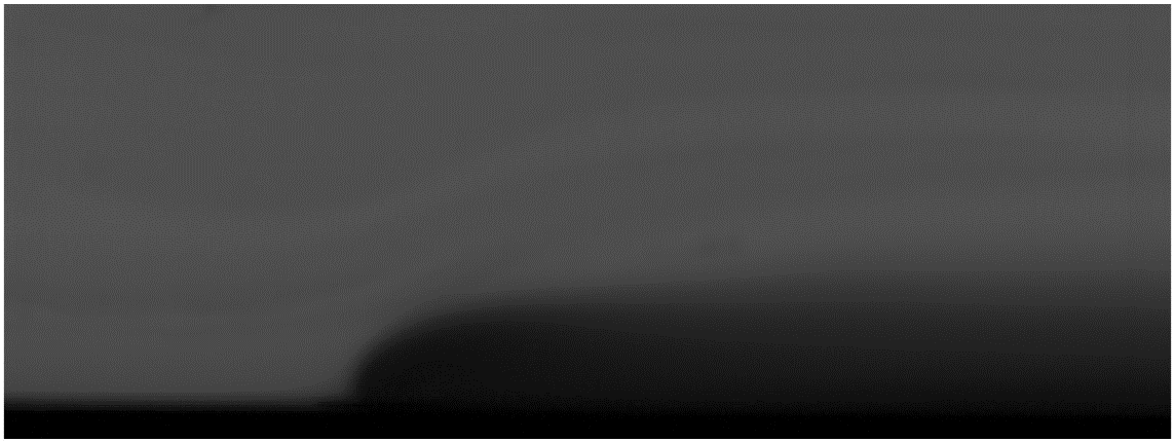

Image 13. Average image.

In Image 14, two lines were drawn to indicate the assumed path that the shock waves created by the shock generator should have followed. This analysis was done with direct imaging and not with Schlieren and that is the reason why the supersonic waves were not captured. The existence of other shock waves in the whole interaction process could not really be known.

Image 14. Image showing the course of the supersonic waves.

To establish the jet boundaries, the image was binarized by selecting a threshold intensity value of 18.5 % (0.185) following the Otsu method to determine the optimal threshold value. This method was effective because the image contained two kinds of pixels, foreground, and background pixels. The process consisted of calculating the histogram of the grayscale image and dividing it into two groups. The optimal threshold value was the one that maximized the variance between the two classes.

Image 15. Binarized image.

The results obtained from the laboratory were:

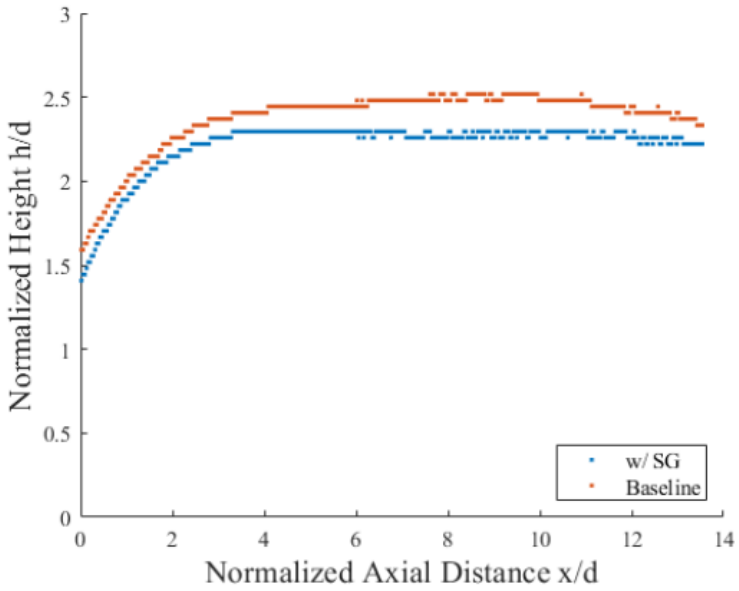

Graph 11. Height penetration fit curves (SG =Shock Generator).

For the calculation of the equations, the curves were fitted to a difference of 150 pixels to show more accurate results. The height penetration equations obtained are:

-Baseline

$$\frac{h}{d} = 2.035 * \left(\frac{x}{d}\right)^{0.126}$$

-With shock generator

$$\frac{h}{d} = 1.92 * \left(\frac{x}{d}\right)^{0.132}$$

The graph shows that the penetration height achieved with the shock generator is lower than in the base case. Two factors must be considered. First, the main shock wave did not impinge on the strong part of the bow shock which likely prevented the formation of a stronger

separation shock that would have promoted the penetration height. In return, the wave indexed on the weakest part of the bow shock and created a transmitted shock because of the interaction with the fluid, which caused the penetration height to be much lower, even below the values of the base case. It should be remembered that the lower the penetration height, the shorter the distance the fluid travels along the axial axis, and the less mixing occurs, which does not help combustion.

Secondly, as seen in Image 14, another shock wave was created at the backside of the wedge. The creation of this supersonic wave may have been the result of the rupture of the boundary layer and the strong turbulence created in the area by the process of air compression and expansion. The final part of the graphs (from x/d =4) shows how the second shock wave created can influence the height of the spray plume to be lower, which is in agreement with what was explained by [31]. This could be due to the small dimensions of the wind tunnel which caused the continuous rebound of the transmitted shock waves. However, no definitive conclusions can be drawn and may be interesting to further analyze how this supersonic wave affects the interaction with the downstream fuel.

To further analyze the difference between the penetration heights in both cases (with or without a shock generator), the two average images were superimposed for comparison.

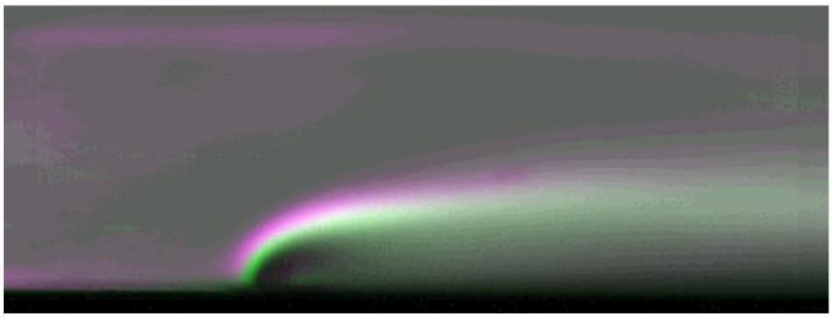

Image 16. Comparison of the standard deviation between baseline and wedge 12º.

In Image 16, it is compared the typical deviations of both photographs. The green color represents larger standard deviation for the shock generator while the magenta represents

larger standard deviation for the baseline data. It shows the differences in height. The green zone is much lower than the purple (baseline). Also, further studies could be made on how the shock wave created from the back of the wedge, affects the mixing downstream as the dispersion is higher when using the wedge when the dimensions of the wind tunnel are small.

It is concluded that, in this case, the shock generator can be a disadvantage in reaching a higher penetration height if it does not impact right in the strong bow shock zone.

Also, it was analyzed the behavior of the penetration height curve obtained in the laboratory with respect to the correlations studied in the Literature review. In the experiment at the University of Minnesota with q = 0.3.

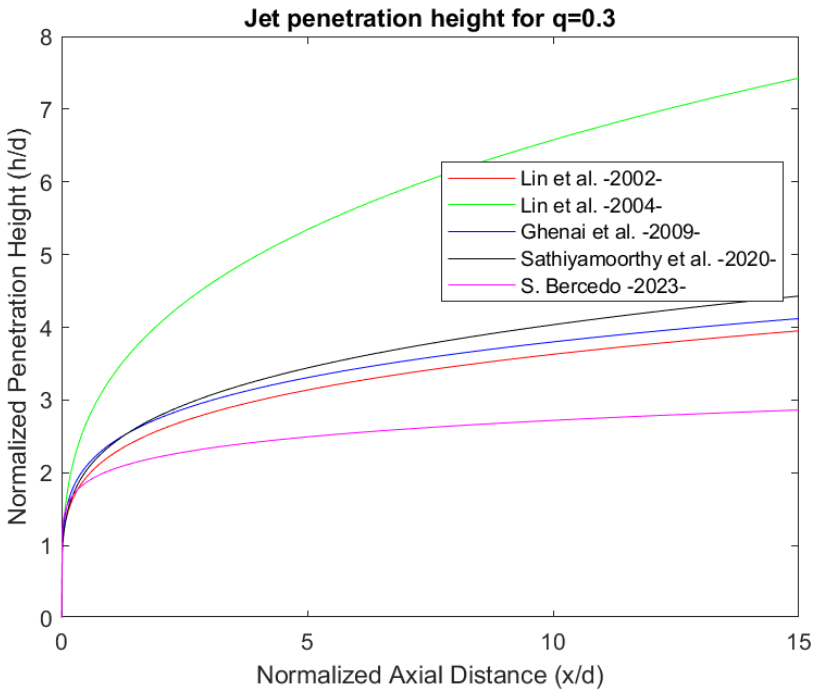

Graph 12. Comparison of penetration height with other studies (q=0.3).

In the baseline case, the penetration height is also a little lower than if compared to the other correlations with a q=0.3. This may be due to the measurement technique used and the jet boundary established or a result of the various disturbances in the wind tunnel that caused supersonic waves to appear.

Moreover, pressure graphs were also obtained from the data collected by the pressure transducers. The signal was decomposed into its frequency components using the Fast Fourier Transform.

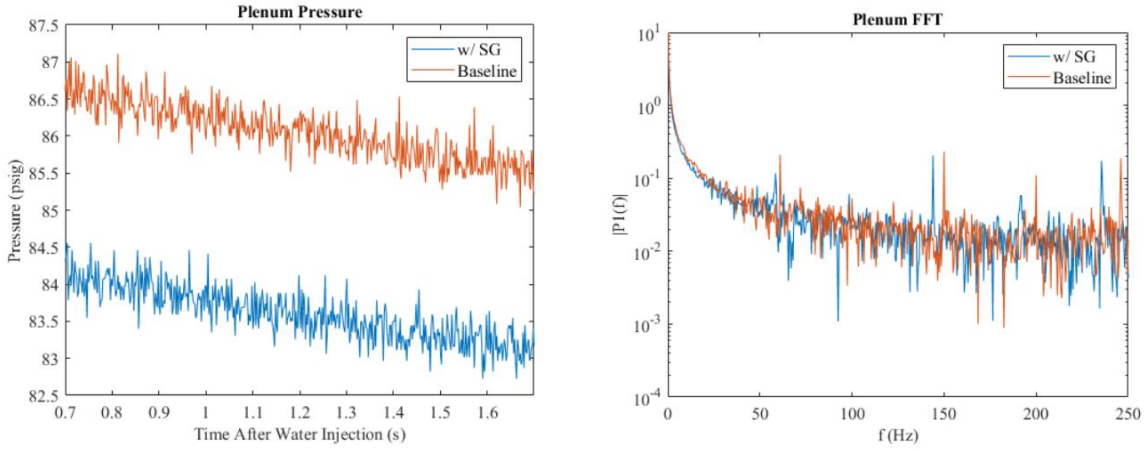

Graph 13. Plenum Pressure and Plenum FFT.

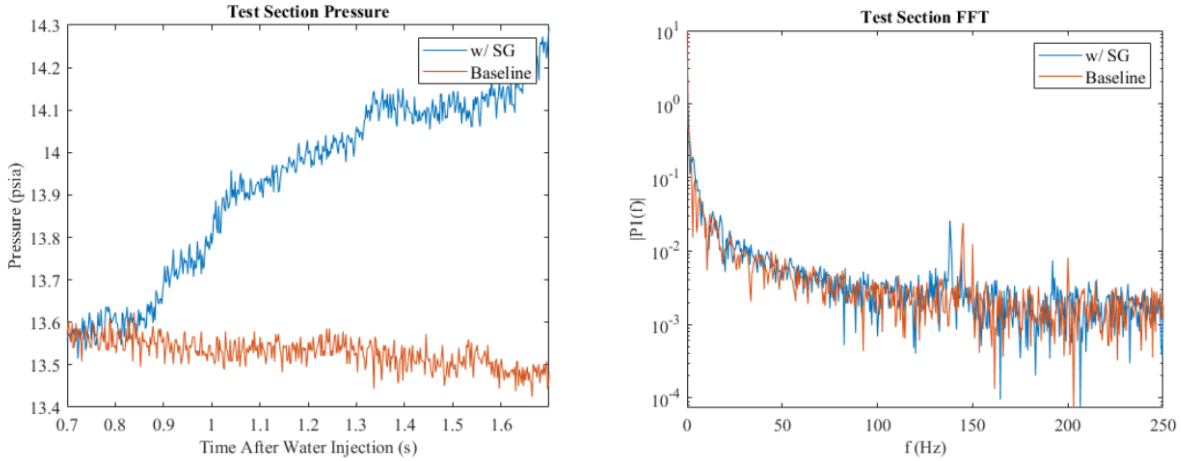

Graph 14. Test Section Pressure and Test Section FFT.

In the first two situations, no significant differences were observed in the frequency signals calculated in the Fourier transform. In the graph showing the data collected in the test section, the pressure when the shock generator is used increases with respect to the baseline. This may be due to the interaction with a shock wave, however, since it has not been possible to use the Schlieren imaging it cannot be confirmed.

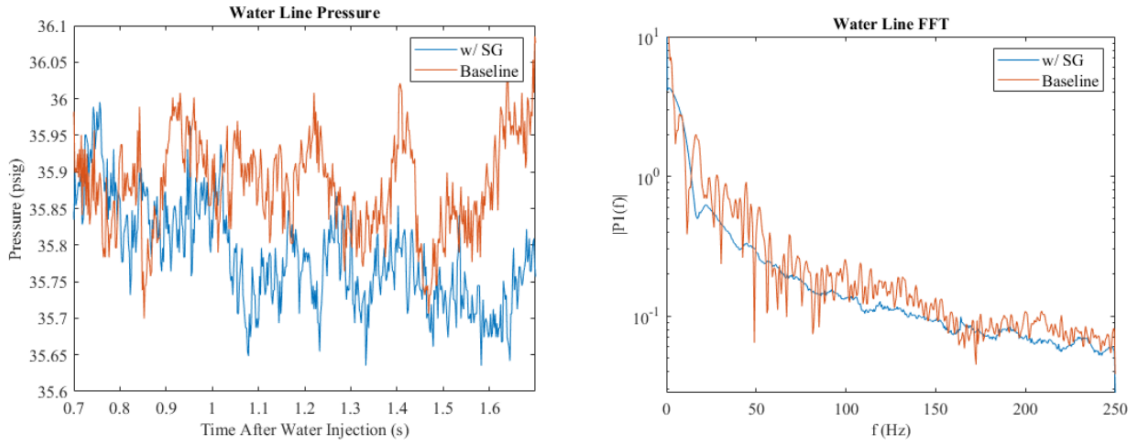

Graph 15. Water Line Pressure and Water Line FFT.

On the other hand, the results obtained with the latest pressure transducer were very interesting. Very pronounced peaks were observed in the pressure data. When calculating the FFT, the base case was much more chaotic than with the shock generator. This could be because the shock generator may have generated an additional shock wave that hit right on top of where the liquid was injected, which could have prevented the rupture of the boundary layer. However, this also cannot be stated because of the lack of conclusions due to the lack of Schlieren imaging.

In conclusion, it is evident that more studies should be carried out on this subject to draw more accurate conclusions.

Chapter 6. CONCLUSIONS AND FUTURE RESEARCH

After analyzing the results, it is evident that much more research needs to be done in this area since it is still difficult to predict the effects that adding a shock generator may have on the atomization process of the liquid. Although the results are different from those obtained by Sebastian *et al.* [5] many factors may have come into play.

First, the geometry and shape of the shock generator. By reducing the dimensions of the wind tunnel in the area where the shock generator was added, the flow became very unstable, and the formation of new shock waves could have affected the penetration height of the fluid. Therefore, it would be interesting to study the influence of the obstruction produced by the shock generator on the flow passage in the process. Also, the measurement systems used, and the jet boundaries established may also have influenced the lower penetration height.

The University of Minnesota is currently working on the design and construction of a new wind tunnel that has a higher precision in its operations and that will have a larger test section that will allow to take the videos through Schlieren Imaging when the shock generator is added and thus be able to study the behavior of the supersonic waves formed.

At the same time, it would be interesting to conduct experiments on the size of the droplets and see what effect supersonic waves have on them when they hit the front and rearmost part of the spray plume. However, this will require new measurement systems such as PDPA.

At the University of Minnesota laboratory, they are also studying how the viscosity of the injected liquid affects the penetration height and therefore the atomization process.

There is still much to be known about scramjet engines and their combustion. Addressing the issue of LJISC - liquid jet in supersonic crossflow - is an essential first step in the development of these new technologies that could be a turning point in the world of aviation.

The addition of a shock generator could bring significant benefits, but much more experimentation and research is needed.

Chapter 7. BIBLIOGRAPHY

[1] Z. Ren, B. Wang, G. Xiang, D. Zhao y L. Zheng, «Supersonic spray combustion subject to scramjets: Progress and challenges.,» *Progress in Aerospace Sciences.*, vol. 105, pp. 40-59, 2019.

[2] C. Ghenai, H. Sapmaz y C. X. Lin, « Characterization of Aerated Liquid Jet in Subsonic and Supersonic Cross Flow.,» *AIAA journal*, 2005.

[3] J. B. Perurena, C. O. Asma, R. Theunissen y O. Chazot, «Experimental investigation of liquid jet injection into Mach 6 hypersonic crossflow.,» *Experiments in Fluids*, vol. 46, nº 3, pp. 403-417, 2009.

[4] C. Segal, Supersonic Combustion Processes, 2009.

[5] D. S. Sebastian, . S. K. Thomas y . T. Muruganandam, «Gas dynamic effects of shock interaction with the liquid jet in supersonic crossflow.,» *AIAA*, 2022.

[6] J. D. Anderson, Fundamentals of Aerodynamics, 2 ed., McGraw-Hill, Inc, 1991.

[7] E. Harrington y G. Galvez, «LibrosMaravillosos,» [En línea]. Available: http://www.librosmaravillosos.com/lahistoriadelaaviacion/index.html. [Último acceso: Febrary 2023].

[8] B. Dunbar, «NASA,» 22 August 2006. [En línea]. Available: https://www.nasa.gov/centers/dryden/espanol/FS-040-DFRC_espanol.html. [Último acceso: 2023].

[9] G. Choubey, . Y. D, W. Huang, L. Yan, H. Babazadeh y K. Pandey, «Hydrogen fuel in scramjet engines - A brief review,» *International Journal of Hydrogen Energy*, vol. 45, pp. 16799-16815, 2020.

[10] C. Segal, The Scramjet Engine: Processes and Characteristics, Cambridge University Press, 2010.

[11] M. Smart, «Scramjets. In Advances on Propulsion Technology for High-Speed Aircraft,» 2008. [En línea]. Available: https://www.sto.nato.int/publications/STO%20Educational%20Notes/RTO-EN-AVT-150/EN-AVT-150-09.pdf.

[12] S. Pachón y F. Rodríguez, «PROPULSION AIR-BREATHING, SCRAMJET,» Fundación Universitaria Los Libertadores, 2012.

[13] N. Das, K. Pandey y K. Sharma, «A brief review on the recent advancement in the field of jet engine - scramjet engine,» *Materials Today: Proceedings*, vol. 45, pp. 6857-6863, 2021.

[14] K. N. Roberts, «ANALYSIS AND DESIGN OF A HYPERSONIC SCRAMJET ENGINE,» University of Texas at Arlington, 2008.

[15] A. Nejad y J. Schetz, «Effects of viscosity and surface tension on a jet plume in supersonic crossflow.,» *AIAA journal*, vol. 22, pp. 458-459, 1984.

[16] K.-C. Lin, P. J. Kennedy y T. A. Jackson, «PENETRATION HEIGHTS OF LIQUID JETS IN HIGH-SPEED CROSSFLOWS.,» *American Institute of Aeronautics & Astronautics*, p. 17, 2002.

[17] C. Mauger, L. Méès, M. Michard, A. Azouzi y S. Valette, «Shadowgraph, Schlieren and interferometry in a 2D cavitating channel flow.,» *Experiments in Fluids.,* vol. 53, pp. 1895-1913, 2012.

[18] K.-C. Lin, P. J. Kennedy y T. A. Jackson, «Structures of Water Jets in a Mach 1.94 Supersonic Crossflow.,» *42nd AIAA Aerospace Sciences Meeting and Exhibit.,* 2004.

[19] B. Doda, «velocimetry.net,» Velocimetry Portal, 2008. [En línea]. [Último acceso: June 2023].

[20] C. Ghenai, H. Sapmaz y C.-X. Lin, «Penetration height correlations for non-aerated and aeratedtransverse liquid jets in supersonic cross flow.,» *Experiments in Fluids,* vol. 46, pp. 121-129, 2009.

[21] K. Sathiyamoorthy, T. H. Danish, V. S. Iyengar, J. Srinivas y X. Harikrishna, «Penetration and Combustion Studies of Tandem Liquid Jets in Supersonic Crossflow,» *Journal of propulsion and power,* vol. 36, nº 6, pp. 920-930, 2020.

[22] J. Lee, K. Lin y D. Eklund., «Challenges in fuel injection for high-speed propulsion systems.,» *AIAA,* vol. 53, pp. 1405-1423, 2015.

[23] Y. Zhou, Z. Cai, Q. Li, C. Li, M. Sun, P. Li y H. Wang, «Review of atomization mechanism and spray characteristics of a liquid jet in supersonic crossflow.,» *Chinese Journal of Aeronautics,* p. 23, 2023.

[24] A. Nejad, J. A. Schetz y A. K. Jakubowski, «Mean droplet diameter resulting from atomization of a transverse liquid jet in a supersonic air stream.,» *AIAA,* p. 72, 1980.

[25] C. Medipati, S. Deivandren y R. Govardhan, «Liquid jet injection in supersonic crossflow: Self-induced jet oscillations and its effects.,» *International Journal of Multiphase Flow,* vol. 158, 2023.

[26] S. Murphy, V. Mortimer y M. Lydon, «Droplet Sizing and Imaging of Agricultural Sprays Using Particle/Droplet Image Analyses.,» *ResearchGate*, pp. 324-329, 2004.

[27] P. Li, Z. Wang, M. Sun y H. Wang, «Numerical simulation of the gas-liquid interaction of a liquid jet in supersonic crossflow.,» *Acta Astronautica*, vol. 134, pp. 333-344, 2017.

[28] C. Li, C. Li, F. Xiao, Q. Li y Y. Zhu, «Experimental study of spray characteristics of liquid jets in supersonic crossflow.,» *Aerospace Science and Technology*, vol. 95, p. 11, 2019.

[29] C.-J. Tam, S. Cox-Stouffer, K.-C. Lin, M. Gruber y T. Jackson, «Gaseous and Liquid Injection into High-speed Crossflows.,» *AIAA*, 2005.

[30] K. A. Sallam, K.-C. Lin, S. Hammack y C. Carter, «Digital Holographic Analysis of the Breakup of Aerated Liquid Jets in Supersonic Crossflow.,» *55th AIAA Aerospace Sciences Meeting*, 2017.

[31] J. Zhao, . Y. Tong, Y. Ren, . Y. Zhu, . Z. Chen, W. Lin y W. Nie, «Structures of liquid jets in supersonic crossflows in a rectangular channel with an expansion section.,» *Physics of Fluids*, vol. 111704, 2020.

[32] E. Erdem, . S. Saravanan, J. Lin y K. Kontis, «Experimental Investigation of Transverse Injection Flowfield at Mach 5 and the Influence of Impinging Shock Wave.,» *AIAA*, 2012.

[33] B. Schmidt, «Schlieren Visualization,» 2015.

APPENDIX I. WIND TUNNEL FACILITIES.

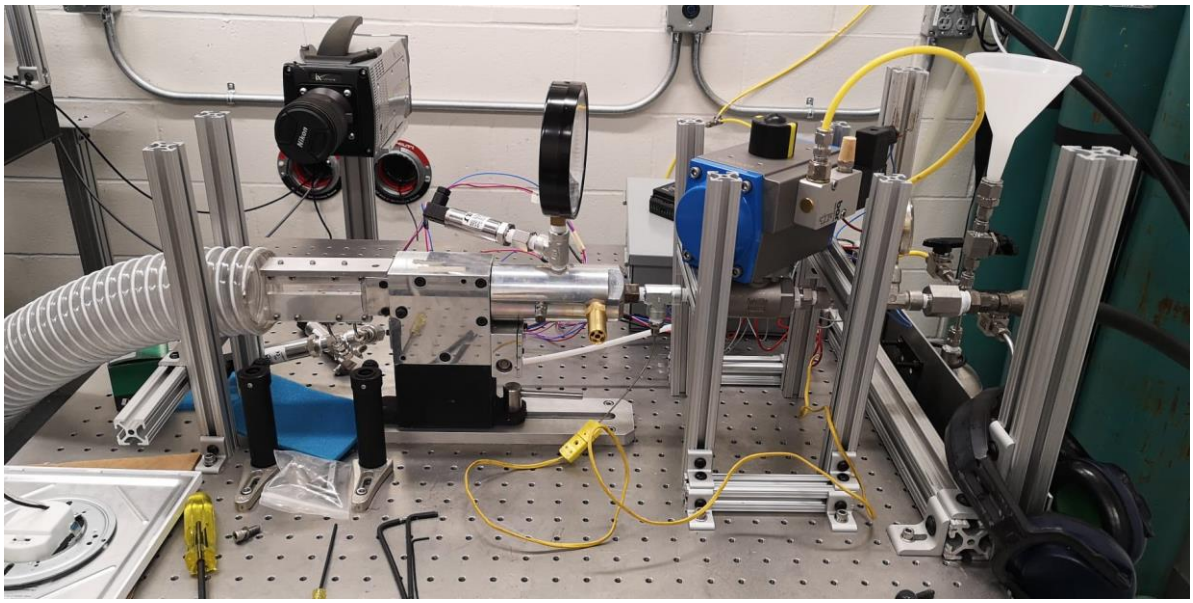

Image 17. Wind Tunnel Facilities.

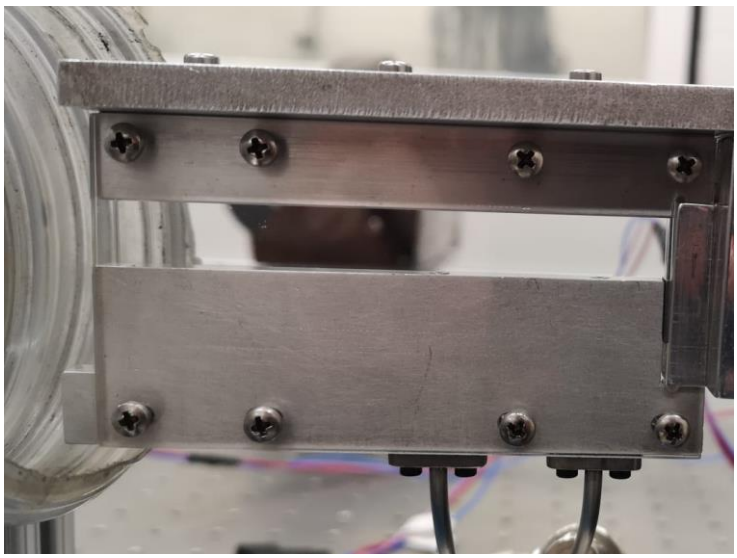

Image 18. Test Section.

Image 19. Light source for Schlieren imaging.

Image 20. IX-727 High-Speed Camera

APPENDIX II. SUSTAINABLE DEVELOPMENT GOALS

The Sustainable Development Goals (SDGs) were born with the aim of achieving a social response to eradicate poverty, safeguard the planet and contribute to the attempt to improve the lives of people around the world. In 2015, the member countries of the United Nations approved seventeen goals to obtain such results fifteen years after their approval. Thus, the project is aligned with some SDGs to contribute to these changes.

Paying particular attention to Objective 9 of the SDG Agenda, this project aims to foster innovation and advance the use of new technologies. The field of hypersonic speeds is still somewhat unknown to society. The conclusions of this study are intended to be a technological breakthrough and can be implemented so that the aeronautical industry can continue to grow and develop. At the same time, the project seeks to maximize the use of fuel and, consequently, of available resources as much as possible.

In the same way, and with a view to the long term, the project is developed in parallel with Objective 3, promoting well-being for all. The search for new, faster and less polluting forms of transport is key to achieving greater comfort for the entire population and contributing to the care and conservation of the planet. These new technologies can be the first step to entering a field yet to be explored, leading to industrial discoveries that will benefit everyone.